Title Page

High levels of heterogeneity in diazotroph diversity and activity within a putative hotspot for marine nitrogen fixation

Lauren F Messer[1*], Claire Mahaffey[2], Charlotte Robinson[1], Thomas C Jeffries[1+], Kirralee G Baker[1], Jaime Bibiloni Isaksson[1], Martin Ostrowski[4], Martina A Doblin[1], Mark V Brown[3], Justin R Seymour[1]

* corresponding author contact: LaurenFrances.Messer@student.uts.edu.au

1 Plant Functional Biology and Climate Change Cluster, University of Technology Sydney, 15 Broadway, Ultimo, NSW, 2007, Australia

2 Department of Earth, Ocean and Ecological Sciences, University of Liverpool, 4 Brownlow Street, Liverpool, L69 3GP, United Kingdom

3 School of Biotechnology and Biomolecular Sciences, University of New South Wales, Sydney, NSW, 2033, Australia

4 Department of Chemistry and Biomolecular Sciences, Macquarie University, Sydney, NSW, Australia

+ Current address: Hawkesbury Institute for the Environment, University of Western Sydney, Richmond, NSW, Australia.

LFM, CM, MVB and JRS conceived the study; LFM, CR, MVB and JRS acquired data; TCJ, KGB, JBI, MO and MAD assisted with data acquisition; LFM analysed the data; LFM, CM, TCJ, MVB and JRS interpreted the data; LFM, MVB and JRS wrote the manuscript; all authors revised the manuscript.

Abstract

Australia's tropical waters represent predicted "hotspots" for nitrogen (N_2) fixation based on empirical and modelled data. However, the identity, activity and ecology of diazotrophs within this region are virtually unknown. By coupling DNA and cDNA sequencing of nitrogenase genes (*nifH*) with size fractionated N_2 fixation rate measurements, we elucidated diazotroph dynamics across the shelf region of the Arafura and Timor Seas (ATS) and oceanic Coral Sea during Austral spring and winter. During spring, *Trichodesmium* dominated ATS assemblages, comprising 60% of *nifH* DNA sequences, while *Candidatus* Atelocyanobacterium thalassa (UCYN-A) comprised 42% in the Coral Sea. In contrast, during winter the relative abundance of heterotrophic unicellular diazotrophs (δ–proteobacteria and γ-24774A11) increased in both regions, concomitant with a marked decline in UCYN-A sequences, whereby this clade effectively disappeared in the Coral Sea. Conservative estimates of N_2 fixation rates ranged from < 1 to 91 nmol L^{-1} d^{-1}, and size fractionation indicated that unicellular organisms dominated N_2 fixation during both spring and winter, but average unicellular rates were up to 10-fold higher in winter than spring. Relative abundances of UCYN-A1 and γ-24774A11 *nifH* transcripts negatively correlated to silicate and phosphate, suggesting an affinity for oligotrophy. Our results indicate that Australia's tropical waters are indeed hotspots for N_2 fixation, and that regional physicochemical characteristics drive differential contributions of cyanobacterial and heterotrophic phylotypes to N_2 fixation.

Keywords: *nifH* amplicon sequencing / seasonal nitrogen fixation / tropical ocean / heterotrophic diazotrophs

Subject category: Microbial ecology and functional diversity of natural habitats

47 Running title: Diazotroph dynamics in the tropical Australian ocean

48

49 INTRODUCTION

50 Biological nitrogen (N_2) fixation is a fundamental process within the ocean, helping to
51 alleviate nitrogen limitation, thereby supporting primary production and the sequestration of
52 carbon to the deep sea (Sohm et al. 2011; Karl et al. 2012). N_2 fixation is mediated by a
53 diverse range of microorganisms (Zehr et al., 2003), including the photoautotrophic
54 cyanobacterium *Trichodesmium*, as well as unicellular cyanobacteria, diatom-associated
55 cyanobacteria and heterotrophic bacteria, all of which are distributed across tropical and
56 subtropical latitudes (Capone et al., 1997, 2005; Montoya et al., 2004; Moisander et al., 2008,
57 2010, 2014; Foster et al., 2009).

58 High rates of marine N_2 fixation have been observed in Australia's tropical waters (Montoya
59 et al., 2004) and N_2 fixation rate models predict rates sometimes exceeding 100 μmol m^{-2} d^{-1}
60 in this region (Luo et al., 2014). Additionally, ecosystem models predict cyanobacterial
61 diazotrophs will be abundant in northern Australian waters (Monteiro et al., 2010). Indeed,
62 *Trichodesmium* has long been recognised as an important member of the phytoplankton in
63 this region (Hallegraeff and Jeffrey, 1984; Burford et al., 1995, 2009), and unicellular
64 diazotrophs are assumed to be highly active here as well (Montoya et al., 2004). However,
65 compared to the South Pacific Ocean, where unicellular diazotrophs including *Candidatus*
66 Atelocyanobacterium thalassa (UCYN-A), *Crocosphaera watsonii,* and the γ-proteobacterial
67 clade γ-24774A11 are known to be abundant (Moisander et al., 2010, 2014), we currently
68 lack any detailed understanding of patterns in the diversity, activity and ecology of
69 diazotrophs within tropical Australian waters.

70 We surveyed two distinct oceanographic provinces in northern Australia, which play
71 important roles in global climate and ocean circulation. These include the semi-enclosed
72 Arafura and Timor shelf sea regions (ATS), which form part of the Indian Pacific Warm Pool

(Alongi et al., 2011), and the open ocean Coral Sea, where the South Pacific western boundary current originates (Qu and Lindstrom, 2002). The ATS is considered autotrophic (McKinnon et al., 2011) and highly productive, particularly during the tropical dry season (Austral winter) (Alongi et al., 2011), despite relatively low surface nitrogen concentrations (< 2 μM nitrate) and no deep-water reservoir of nutrients (Lyne and Hayes, 2005). Annual primary production in the Coral Sea is relatively low and nitrogen limitation is predicted (Condie and Dunn, 2006), with the upper 100 m of the water column being highly oligotrophic throughout the year (Lyne and Hayes, 2005).

N_2 fixation has been found to be a significant biogeochemical feature of this important region of the ocean (Montoya et al., 2004; Luo et al., 2014), but we observed substantial physicochemical variability, manifest in differential temperature and salinity signatures and nutrient availability, between the ATS and Coral Sea, which may influence the relative importance of diazotroph activity, particularly given the highly dynamic nature of diazotroph communities (Robidart et al., 2014). By combining *nifH* sequencing and size fractionated $^{15}N_2$ rate measurements, we assessed spatial and temporal patterns in the diversity and activity of N_2 fixing bacteria across this region, with the aim of characterising the dynamics of diazotrophy within this putative global N_2 fixation hotspot.

MATERIALS AND METHODS

Sample Collection

Sampling was performed during two voyages aboard the *R/V Southern Surveyor,* consisting of a 2500 km transect from Darwin to Cairns conducted in the Austral spring (October 2012;

ss2012_t07; Figure 1A), and a 5000 km transect from Broome to Brisbane during the Austral winter (July-August; ss2013_t03; Figure 1B). October marks the beginning of the tropical wet season, while the July-August period corresponds to the middle of the dry season.

Seawater was sampled daily at dawn during both transects for diazotroph diversity (DNA) and gene expression (cDNA) analyses and N_2 fixation rate measurements, as well as mid-afternoon for analysis of diazotroph diversity (DNA) only, resulting in stations separated by 100 - 300 km. Samples were collected from the surface at all stations, and the chlorophyll maximum (cmax) when a fluorescence peak was discernible in the water column (see Supplementary Information).

N_2 fixation rates

Net $^{15}N_2$ assimilation (Montoya et al., 1996) was measured to obtain estimates of N_2 fixation by the whole community (WC) and < 10 μm unicellular size fraction (USF) of diazotrophs as previously described (Church et al. 2009; see Supplementary Information). Experiments conducted with surface and cmax samples were incubated at *in situ* temperature and light levels for 24 h and terminated by filtration (see Supplementary Information). Assimilation rates were calculated as previously described (Montoya et al. 1996), based on a theoretical enrichment of ca. 8 atom% $^{15}N_2$, and are considered conservative estimates of N_2 fixation due to the known incomplete dissolution of the $^{15}N_2$ gas bubble (Mohr et al., 2010).

Nucleic acid collection and extraction

At each station, 4-8 L of seawater was filtered through 0.22 μm Sterivex filter units (EMD Millipore, Billerica, MA, USA). Filters were immediately frozen in liquid nitrogen and stored

119 at -80°C. Community DNA was extracted using the PowerWater DNA Extraction Kit
120 (MoBio Laboratories, Carlsbad, CA, USA) according to the manufacturer's instructions,
121 including an additional 10 min heating step with solution PW1 to ensure complete cell lysis.
122 DNA yield was quantified using a Broad Range DNA Qubit™ Assay (Invitrogen, Carlsbad,
123 CA, USA) with a Qubit™ 2.0 Fluorometer.

124 RNA samples were collected from all N_2 fixation incubation stations. Seawater (1-2 L) was
125 filtered through a 0.22 µm Durapore membrane filter (Millipore) within 15 minutes of
126 collection, after which RNAlater solution (300 µl; Ambion, Austin, TX, USA) was added and
127 filters were frozen in liquid nitrogen and stored at -80°C. Total RNA was extracted as
128 previously described (Frias-Lopez et al. 2008; Stewart et al. 2010; see Supplementary
129 Information).

130

131 *nifH* PCR amplification and amplicon pyrosequencing

132 A nested PCR protocol was used to amplify an ~359 bp region of the nitrogenase gene, using
133 the degenerate primers: nifH3, nifH4, nifH1 and nifH2 (Zani et al., 2000; Zehr and Turner,
134 2001). Equal volumes of DNA or cDNA were used as template (2 µl) in the first stage of the
135 reaction, and 1 µl of PCR product was used as template in the second stage, using previously
136 described reaction conditions (Messer et al. 2015; see Supplementary Information).

137 The *nifH* amplicons were sequenced using the 454 FLX Titanium pyrosequencing platform
138 (Roche, Molecular Research LP, USA) following an additional 10 PCR cycles with custom
139 barcoded nifH1 and nifH2 primers under the same PCR reaction conditions (Dowd et al.
140 2008; Farnelid et al. 2011, 2013; Messer et al. 2015; Supplementary Information). Raw
141 sequences were quality filtered, whereby sequences with a quality score < 25 and reads < 200

142 bp long were removed, and clustered into operational taxonomic units (OTUs) at 95%
143 sequence identity (Penton et al., 2013) using UCLUST (Edgar, 2010) and rarefied to the
144 lowest number of sequences per sample (872 sequences) in QIIME (Caporaso et al., 2010).
145 To assign putative taxonomy, representative sequences from *nifH* OTUs were aligned to the
146 closest sequence in a custom *nifH* database (updated in April 2014) (Zehr et al., 2003; Heller
147 et al., 2014) and placed in a phylogenetic tree using the maximum parsimony tool in ARB
148 (Westram et al., 2011). Translated *nifH* sequences were compared to the Ribosomal Database
149 Project's *nifH* protein database using FrameBot from the Fungene pipeline (Fish et al., 2013;
150 Wang et al., 2013).

151

152 Statistical analyses

153 Rarefied sequence data were square-root transformed and a resemblance matrix generated
154 using Bray-Curtis similarity. Environmental parameters (Supplementary Table 1) were
155 normalised and a resemblance matrix generated using Euclidean distance (Clarke and
156 Warwick, 2001). Statistical analyses, including analysis of similarities (ANOSIM; Clarke
157 1993), distance based linear modelling (DistLM) and distance-based redundancy analysis
158 (dbRDA) (Legendre and Anderson, 1999; McArdle and Anderson, 2001), were performed in
159 the PRIMER + PERMANOVA software package (v6; Clarke & Warwick 2001).

160 In order to identify associations (linear regression, p) between N_2 fixation rates, expressed
161 *nifH* OTUs and environmental parameters, we calculated the maximal information coefficient
162 (MIC) between all variable (n = 255) pairs from all samples (n = 28) using the MINE
163 statistics package (Reshef et al., 2011). Strongly co-linear variables ($p > 0.9$ or > -0.9) were
164 removed from the analyses. After correction for multiple testing (Benjamini and Hochberg,
165 1995), statistically significant co-occurrence relationships ($P < 0.01$; $MIC > 0.473$) between

pairs of variables were input into Cytoscape v 2.8 (Smoot et al., 2011) and used to generate network diagrams for visualisation.

RESULTS

Physicochemical characteristics of the ATS and Coral Sea

During both spring and winter, ATS waters were warmer, exhibited lower salinities and had higher nutrient concentrations and phytoplankton abundances than Coral Sea waters (Figure 1, Supplementary Table 1). Mean sea surface temperature (SST) in the ATS was 27.4 °C in spring and 26.4 °C in winter, compared with 26.5 °C and 24.3 °C in the Coral Sea. During both sampling periods, salinity increased from 33.5 to > 35 PSU at a longitude of approximately 143 °E, reflecting the transition from the shelf region (ATS) to the open ocean (Coral Sea) (Figure 1). Mean nitrate and phosphate concentrations were greatest during the spring, being 3.5 and 3.8 times greater in the ATS than the Coral Sea respectively, with this discrepancy falling to 2.6 and 1.8 times in the winter. N:P ratios were always < 16:1 indicating an excess of phosphate compared to nitrate and ammonium, particularly in surface waters (Supplementary Table 1). We also observed intra-region nutrient differences, for example silicate concentrations were highest in the eastern region of the ATS in spring (5.97 μmol L^{-1}; SS7), and the western region in winter (5.74 μmol L^{-1}; WS1; Figure 1). Pigment analyses indicated that phytoplankton communities within the ATS were dominated by microphytoplankton such as diatoms, whereas pico- and nanophytoplankton were relatively more abundant in the Coral Sea (Supplementary Table 1).

189 N_2 fixation rates

190 N_2 fixation rates within the WC and USF ranged from < 1 to 91 nmol L^{-1} d^{-1}, and at times
191 displayed substantial variability between the ATS and Coral Sea and between seasons (Figure
192 2). During the Austral spring, mean WC N_2 fixation rates (± sd.) were 23 ± 32 nmol L^{-1} d^{-1}
193 compared to 6 ± 7 nmol L^{-1} d^{-1} in the USF. However, it is notable that the majority of N_2
194 fixation occurred within the < 10 μm size class at three out of four ATS sites (Figure 2A).
195 Within ATS waters there was a peak in N_2 fixation at site SS5 where WC rates reached 71 ±
196 10 nmol L^{-1} d^{-1}, significantly greater than the USF rates of 16 ± 3 nmol L^{-1} d^{-1} (One-way
197 ANOVA, Tukey HSD, $P < 0.05$). This was the only ATS site sampled for N_2 fixation rate
198 measurements where a cmax was observed, and rates within it were comparatively low at ≤ 4
199 nmol L^{-1} d^{-1} for both size classes (Figure 2A).

200 Spring N_2 fixation rates in the Coral Sea were lower than in the ATS, with mean rates of 13 ±
201 5 (WC) and 7 ± 6 nmol L^{-1} d^{-1} (USF). However, within this region the contribution made by
202 unicellular organisms was higher, being ~50% of the total. Rates in Coral Sea surface waters
203 reached a maximum of 18 ± 2 (WC) and 14 ± 13 (USF) nmol L^{-1} d^{-1} at SS16 (Figure 2A). N_2
204 fixation rates in the cmax were at times higher than in the surface waters, reaching up to 24 ±
205 0.6 (WC) and 18 ± 5 (USF) nmol L^{-1} d^{-1} (Figure 2A).

206 A marked increase in N_2 fixation was observed in both regions during the Austral winter
207 (Figure 2B). Within ATS surface waters, WC N_2 fixation increased almost three-fold in
208 winter, with a mean of 60 ± 15 nmol L^{-1} d^{-1} across the six sites. Furthermore, the majority of
209 this activity was attributable to the USF (One-way ANOVA, Tukey HSD, $P > 0.05$), such that
210 mean USF rates increased almost ten-fold in winter to 57 ± 23 nmol L^{-1} d^{-1}. Maximum rates
211 recorded in the ATS surface waters were similar to the spring (Figure 2). Only one winter

ATS site had a discernible cmax and here, in contrast to the spring, N_2 fixation was also relatively high (Figure 2B).

Mean winter N_2 fixation rates in the Coral Sea were four and seven-times higher than during the spring in the WC (56 ± 32 nmol L^{-1} d^{-1}) and USF (47 ± 28 nmol L^{-1} d^{-1}) respectively. While mean N_2 fixation rates were again lower in the Coral Sea than the ATS, the maximum rates recorded in Coral Sea surface waters were the highest observed, reaching 91 ± 7 (WC) and 71 ± 18 nmol L^{-1} d^{-1} (USF) at station WS16, towards the southern end of the transect (Figure 2B). During the winter, four Coral Sea sites had discernible cmax, where N_2 fixation rates were also relatively high (Figure 2B).

Diazotroph population dynamics in ATS and Coral Sea waters

A total of 174 *nifH* OTUs were resolved from our samples. Phylogenetic analysis revealed the presence of photoautotrophic, photoheterotrophic and heterotrophic diazotrophs during both transects, and these clustered with environmental *nifH* sequences originating from the Pacific and Atlantic Oceans and the South China Sea (Supplementary Figure 1).

Three *nifH* OTUs were dominant across the data-set, comprising 67% of total *nifH* DNA sequences retrieved. These included OTU6956, which was 100% identical to *Trichodesmium erythraeum* (IMS 101; hereafter *Trichodesmium*) in *nifH* amino acid (aa) composition, OTU6352, which was 100% identical in aa composition to UCYN-A and clustered with the UCYN-A1 ecotype (Supplementary Figure 1), and OTU4713, which shared 91% similarity in aa composition to the γ-proteobacteria *Pseudomonas stutzeri,* and clustered within the γ–24774A11 clade (Moisander et al., 2008, 2014). Despite the ubiquity of these dominant OTUs, significant partitioning of diazotroph population structure was observed between the

ATS and Coral Sea (Figure 3; ANOSIM, Global R: 0.471, $P < 0.001$) and between the Austral spring and winter sampling (ANOSIM, Global R: 0.399, $P < 0.001$). No significant differences were observed between surface and cmax diazotroph communities.

During the Austral spring, *Trichodesmium* comprised 60% of *nifH* sequences in the ATS, and at some sites reached over 80% of sequences in both the surface and cmax (SS3 and SS5 respectively; Figure 3A, B). γ-24774A11 was also detected throughout the ATS during the spring, where it represented 14% of total sequences, and reached a maximum abundance of over 40% of the diazotroph population at SS8 and SS6 (surface and cmax respectively; Figure 3A, Supplementary Figure 2).

In contrast, the Coral Sea was dominated by the unicellular cyanobacterium UCYN-A during the spring. UCYN-A1 was conspicuously absent from the ATS samples, but comprised 42% of the total *nifH* sequences in the Coral Sea, with a maximum abundance of 77% at SS16 (Figure 3A). Like the ATS, γ-24774A11 was also a significant feature of Coral Sea springtime diazotroph populations, where it constituted 21% of sequences, and reached up to 34 and 46% of diazotrophs at the surface and cmax at SS13 and SS14 respectively (Figure 3A; Supplementary Figure 2).

During the Austral winter, *Trichodesmium* still generally dominated throughout the ATS, representing 35% of total *nifH* sequences, but there was an increase in the relative number of heterotrophic diazotrophs compared to the spring (Figure 3). The putative heterotrophic δ-proteobacterial OTUs 359, 7075, and 811, which shared between 96 and 99% aa identity to *Desulfuromonas acetoxidans,* collectively comprised 19% of total sequences, and up to 55% of the diazotroph population in ATS surface waters (Figure 3C; Supplementary Figure 2). Notably these OTUs only accounted for 7% of diazotrophs in the ATS during the spring (Supplementary Figure 2).

Sequences associated with heterotrophic diazotrophs also increased during the winter in the Coral Sea, relative to the spring (Figure 3C, D). However, here they were primarily associated with γ-24774A11, which represented 34% of wintertime Coral Sea *nifH* sequences, reaching a maximum of 64% of diazotrophs at the surface, and 43% at the cmax (Figure 3C, D). In contrast to the spring sampling where they dominated, UCYN-A sequences only comprised 3% of Coral Sea diazotrophs during the winter and remained absent from the ATS (Supplementary Figure 2).

Patterns in *nifH* expression

Consistent with DNA profiles, *Trichodesmium*, UCYN-A1 and γ-24774A11 dominated *nifH* transcripts across the data-set (Figure 4), and significant differences were observed between transcription profiles from the ATS and Coral Sea (ANOSIM, Global R: 0.595, $P < 0.01$). In ATS surface waters, *Trichodesmium* (OTU6956) and γ-24774A11 (OTU4713) dominated *nifH* transcripts during the spring. Specifically, *Trichodesmium* comprised up to 86% of transcripts at sites where high rates of N_2 fixation attributable to the > 10 μm size class were recorded (SS5, Figure 4A). γ-24774A11 represented up to 52% of transcripts during the spring transect (SS8; Figure 4A), even though unicellular N_2 fixation was recorded at relatively low levels (< 1 nmol L^{-1} d^{-1}; Figure 2A).

Within Coral Sea surface waters in spring, *nifH* transcripts mainly consisted of *Trichodesmium*, UCYN-A and γ-24774A11 (Figure 4A). While *Trichodesmium* transcripts decreased throughout the Coral Sea, UCYN-A1 transcripts increased from 4 to 39%, towards southern latitudes where the peak in Coral Sea springtime N_2 fixation was observed (Figure 4A; Figure 2A). Transcripts associated with γ-24774A11 were most abundant in cmax

samples, where they represented up to 71% of expressed *nifH* genes (Figure 4B), although cmax N_2 fixation rates were relatively low (< 1 nmol L^{-1} d^{-1}; Figure 2A).

Similar to the spring sampling, *Trichodesmium* transcripts were often highly abundant in ATS surface waters during the winter, accounting for 98% of transcripts at station WS3 (Figure 4C). Two additional OTUs, OTU1924 and OTU798, also constituted a significant fraction (up to 76 and 67%) of transcripts in the ATS, however these OTUs shared only 20 and 25% aa identity respectively with available *nifH* sequences, with closest matches to members of the Firmicutes. Interestingly, transcripts associated with γ-24774A11 and UCYN-A were not detected in the ATS during the winter (Figure 4C) despite high unicellular N_2 fixation rates (Figure 2B).

In contrast to the spring, where cyanobacterial transcripts were dominant, *nifH* expression in Coral Sea surface waters was more variable during the winter. For example, both γ-24774A11 and OTU7453, which shared 98% aa identity with the cyanobacterium *Mastigocladus laminosus,* contributed up to ~56% of *nifH* transcripts at stations where unicellular N_2 fixation rates were high (WS15 and WS16 respectively; Figure 4C; Figure 2B). Notably, no transcripts associated with UCYN-A ecotypes were detected in Coral Sea surface waters during the winter, but all three ecotypes were present in transcripts from the cmax, along with *Trichodesmium*, γ-24774A11, and some additional cyanobacterial diazotrophs (Figure 4C, D).

Potential drivers of diazotroph populations and activity

Analysis of the diazotroph populations using both *nifH* DNA (Figure 5A) and cDNA (Figure 5B) data indicated clear separation between ATS and Coral Sea regions. DistLM identified

SST and salinity as significant explanatory variables ($P < 0.05$), reflecting the increase in salinity and decrease in temperature associated with the Coral Sea region (Figure 1, Figure 5A, B; Supplementary Table 2). Dissolved silicate and phosphate were also significant ($P < 0.05$) explanatory variables in both the DNA and cDNA DistLM analysis, as were the photoprotective and photosynthetic carotenoids alloxanthin and fucoxanthin ($P < 0.05$), all of which exhibited higher relative concentrations in the ATS compared with the Coral Sea. Interestingly, dissolved oxygen and divinyl chlorophyll *a* were significant ($P < 0.05$) explanatory variables within the *nifH* DNA model but not within the *nifH* cDNA model (Figure 5A, B). However for both models, > 50% of the total variation between diazotroph populations remained unexplained.

Network analysis revealed that N_2 fixation by the USF exhibited a significant, but only moderately strong, negative correlation to ammonium concentration ($p = -0.43$; MIC strength = 0.66; $P < 0.01$), and was also negatively correlated to the relative abundance of UCYN-A2 transcripts ($p = -0.33$; MIC strength = 0.71; $P < 0.01$), possibly reflecting the relatively low abundance of this ecotype (Supplementary Figure 2). N_2 fixation was not significantly correlated to any other environmental parameters or *nifH* OTUs.

A number of *nifH* OTUs were negatively correlated with phosphate and silicate (Figure 6A, B), including two of the most abundant diazotrophs, OTU4713 from the γ-24774A11 clade, and OTU6352 from the UCYN-A1 ecotype. These γ-24774A11 and UCYN-A1 OTUs were also positively correlated to salinity, to each other, and a range of other *nifH* OTUS including the UCYN-A2 (OTU83) and UCYN-A3 (OTU2020), and other γ-24774A11 OTUs (OTU2710 and OTU454; Figure 6C, D; Supplementary Figure 1). No significant correlations were observed between *nifH* transcripts and the concentration of dissolved inorganic nitrogen species.

329

330

331 DISCUSSION

332 Identifying the factors that influence the composition and activity of diazotrophs is key to
333 understanding the relative importance of N_2 fixation on local and global scales (Zehr and
334 Kudela, 2011; Robidart et al., 2014). N_2 fixed by diverse diazotrophic taxa may have
335 different fates within the marine environment (Glibert & Bronk 1994, Mulholland 2007,
336 Foster et al. 2011, Karl et al. 2012, Benavides et al. 2013) and therefore characterisation of
337 the composition of active N_2 fixing assemblages, combined with size fractionated N_2 fixation
338 rates, is necessary to determine the differential contribution of newly fixed N to pelagic
339 ecosystems. Here we report changes in the biogeographical distribution and activity of
340 diazotrophs across a broad tropical region, which has been identified as a potential global
341 "hotspot" for marine N_2 fixation (Montoya et al., 2004; Monteiro et al., 2010; Luo et al.,
342 2014).

343 Previously, Montoya et al. (2004) reported rates of USF N_2 fixation up to 480 nmol L^{-1} d^{-1} in
344 ATS waters (25 m below surface) during the Austral spring. Herein, we sampled during both
345 spring and winter, at similar latitudes (within 0 - 1 °S) and longitudes (within 0.3 – 2 °E), yet
346 observed maximum USF rates that were substantially less than those reported by Montoya et
347 al. (2004). Recently, Raes et al. (2014) reported mean WC rates of ~36 nmol L^{-1} d^{-1} within
348 the westerly region of the ATS during the Austral spring. While not directly comparable due
349 to methodological differences (Wilson et al., 2012), these values are in line with those we
350 measured in the same region during the Austral winter, suggesting relatively high rates are
351 maintained here across seasons. Based on methodological comparisons, there appears to be
352 no clear trend in the level of N_2 fixation rate underestimation using the Montoya et al. (1996)

353 method, due to multiple factors influencing the dissolution of the $^{15}N_2$ bubble (Mohr et al.,
354 2010; Großkopf et al., 2012). However, comparisons made in the North Pacific and Atlantic
355 Oceans indicate that this method could lead to N_2 fixation underestimates of 50 % (Wilson et
356 al. 2012; Benavides et al. 2013), or greater depending on the composition of the diazotroph
357 community (Großkopf et al., 2012).

358 Compared with near surface waters of similar latitudes, including the tropical western South
359 Pacific (< 1 nmol L^{-1} d^{-1}; Moisander et al. 2010), western equatorial Pacific (< 40 nmol L^{-1} d^{-1};
360 Bonnet et al. 2009), eastern tropical South Pacific (ca. ≤ 1 nmol L^{-1} d^{-1}; Dekaezemacker et
361 al. 2013), and the tropical South Pacific Gyre (≤ 3 nmol L^{-1} d^{-1}; Raimbault & Garcia 2008),
362 the maximum conservative rates of N_2 fixation reported here during the Austral winter (91
363 nmol L^{-1} d^{-1}) are relatively high. Indeed, our observations, along with those previously
364 reported (Montoya et al., 2004; Raes et al., 2014) support the proposition that the tropical
365 waters of northern Australia are a "hotspot" of diazotroph activity within the Southern
366 Hemisphere. However, our data also demonstrate significant temporal and spatial variability
367 in N_2 fixation in this region, which we propose is driven by the highly dynamic and
368 heterogeneous nature of the resident diazotroph populations.

369 Across our data-set, the majority of N_2 fixation activity was observed within the USF, and
370 USF N_2 fixation rates were greater in winter than spring, with mean rates ten-times higher in
371 the ATS and seven-times greater in the Coral Sea. While it must be noted that *Trichodesmium*
372 is known to release some of the N_2 it fixes as dissolved organic nitrogen (Glibert and Bronk,
373 1994), and therefore a proportion of ^{15}N-N_2 fixed could have been transferred to the USF
374 during the incubation, these increased USF rates occurred in parallel to an increase in the
375 relative abundance of δ– and γ–proteobacterial *nifH* sequences and γ-24774A11 *nifH*

376 transcripts. This highlights the potential importance of heterotrophic diazotrophs to
377 biogeochemical cycling during the winter across these two quite different regions.

378 This study provides the first detailed characterisation of active diazotroph populations
379 throughout northern Australia. It must be noted that amplicon sequencing approaches can
380 only reconcile relative abundances, and therefore do not allow for the absolute quantification
381 of colonial versus single-celled diazotrophs, and that it is difficult to directly equate
382 diazotroph communities to N_2 fixation activity. However, we identified a range of
383 photoautotrophic, photoheterotrophic and heterotrophic bacteria which share high similarities
384 in *nifH* sequences to those recovered from similar oceanic environments (e.g. Langlois et al.
385 2005; Bombar et al. 2013; Moisander et al. 2010; Thompson et al. 2014; Moisander et al.
386 2014).

387 Despite its shelf sea nature, ATS diazotroph communities typically resembled those of
388 similar latitudes, such as the tropical Atlantic Ocean, where *Trichodesmium* dominates
389 (Langlois et al., 2005; Foster et al., 2009; Goebel et al., 2010). However, heterotrophic
390 groups were also a feature of ATS communities, and we observed a shift from
391 γ–proteobacterial to δ-proteobacterial phylotypes between spring and winter. Conversely,
392 Coral Sea communities contained a greater diversity of cyanobacterial phylotypes, including
393 ecotypes of UCYN-A alongside a lower frequency of *Trichodesmium* sequences, as well as
394 heterotrophic diazotrophs. The composition of Coral Sea diazotroph populations appears
395 similar to those found within the wider tropical and subtropical South Pacific (Moisander et
396 al., 2010, 2014; Halm et al., 2012). However, a seasonal shift in the composition of Coral Sea
397 populations was also observed, such that the relative abundance of UCYN-A ecotypes
398 decreased while γ–24774A11 increased between spring and winter respectively. Previously,
399 Moisander et al. (2014) reported the distribution of γ–24774A11 to be ubiquitous and

relatively homogeneous in South Pacific surface waters during the Austral autumn. By examining spatial and temporal patterns in diazotroph community dynamics, we show that the distribution and relative abundance of γ–24774A11 is variable and that the significance of this group may increase during the Austral winter.

Surprisingly, no significant differences between surface and cmax diazotroph communities were observed in the present study, with *Trichodesmium*, UCYN-A1 and γ–24774A11 sequences all detected down to 120 m below surface. Previously, *Trichodesmium* and unicellular diazotrophs have been shown to have differential depth distributions in the western South Pacific Ocean, with *Trichodesmium* and γ–24774A11 most abundant in upper euphotic zone waters and UCYN-A more abundant deeper within the water column (Moisander et al., 2010, 2014). We found that all three of these groups were relatively abundant in both surface and cmax waters depending on the sampling region and season. We also detected *nifH* expression by *Trichodesmium* 90 m below surface, and UCYN-A1 and γ–24774A11 100 m below surface, indicating that all three groups were active at depth too. This suggests that the physicochemical variables identified to be potential drivers of diazotroph distribution in the present study, were most relevant over horizontal rather than vertical scales, which could be due to similarities between surface and cmax physicochemical signatures (Supplementary Table 1).

The differences in diazotrophic taxa and N_2 fixation activity observed between the ATS and Coral Sea during both seasons are likely attributable to the observed physicochemical conditions, including higher SST, lower salinities and higher nutrient concentrations in the ATS compared with the Coral Sea, features which are characteristic of the study regions (Condie and Dunn, 2006; Alongi et al., 2011; Ceccarelli, 2011). In particular, SST was identified as a strong indicator of the dominant diazotrophic taxa in our study regions. We

observed that *Trichodesmium* dominated communities in the warmer waters of the ATS, displaying maximum relative abundances when SST was > 27 °C, while UCYN-A dominated communities in the cooler Coral Sea waters, although maximum relative abundances of UCYN-A1 transcripts occurred when SST was ~26 °C during the spring. Previously, UCYN-A have been shown to occur at specific temperature optima between 24-26 °C in the western South Pacific (Moisander et al., 2010, 2014). In contrast, during the cooler winter sampling, when SST in the Coral Sea was closer to 24 °C, we observed an increase in relative abundances of γ-24774A11, while the relative abundance of UCYN-A decreased substantially. Maximum relative abundances of γ-24774A11 occurred where SST was ~25 °C, and maximum γ-24774A11 *nifH* expression occurred at 25.8 °C, suggesting a temperature optima around 25-26 °C for this group. Recently, the occurrence of the γ-24774A11 clade has been found to be positively, non-linearly correlated with temperature, with maximum abundances associated with surface waters > 26 °C (Moisander et al., 2014). Overall, our data are consistent with the observed distributions of these organisms across a range of oceanic provinces (Capone et al., 1997; Mazard et al., 2004; Langlois et al., 2008; Moisander et al., 2010), and supports previous findings that temperature is an important determinant of diazotroph spatiotemporal dynamics.

Dissolved silicate and phosphate concentrations, and the concentration of the pigments alloxanthin and fucoxanthin, were also identified as significant discriminating factors explaining some of the heterogeneity between ATS and Coral Sea diazotroph populations. Whether these correlations indicate a direct or indirect effect on diazotroph abundance and consequently N_2 fixation is unclear. Despite high silicate concentrations and pigment indications of diatom dominated phytoplankton communities in the ATS, only one OTU associated with the heterocystous cyanobacterial symbiont of diatoms, *Richelia*, was observed in our sequence data, and this represented a total of only 6 *nifH* sequences (data not

449 shown). The significant negative correlation observed between silicate and UCYN-A1 and γ-
450 24774A11 transcripts, and UCYN-A1 and fucoxanthin, could be indicative of shifting
451 phytoplankton communities between the ATS and Coral Sea, given that UCYN-A is known
452 to live in association with a prymnesiophyte host (Thompson et al., 2012; Hagino et al., 2013;
453 Krupke et al., 2013). Currently, the lifestyle (e.g. free-living, particle attached, or symbiont)
454 of γ-24774A11 remains unknown (Langlois et al., 2015), however it has been speculated that
455 it may depend upon phytoplankton produced dissolved organic carbon (Moisander et al.,
456 2012, 2014). While strongly co-linear variables were removed from our analyses, silicate was
457 inversely correlated to salinity and positively correlated to temperature, so therefore it could
458 also be indicative of a water mass tracer rather than a biological causation.

459 Conversely, phosphate availability is known to directly influence N_2 fixation and *nifH*
460 expression in natural populations of diazotrophs (Sañudo-Wilhelmy et al., 2001; Rees et al.,
461 2006; Turk-Kubo et al., 2012), as well as the oceanic distribution of diazotrophs in general
462 (Sohm et al., 2011). In the present study, phosphate concentrations were relatively high (e.g.
463 0.27 and 0.26 μmol L^{-1}) in the ATS where *Trichodesmium* and δ-proteobacterial dominated
464 communities were observed. In contrast, in the Coral Sea, where UCYN-A1 and γ-24774A11
465 dominated communities, phosphate concentrations were comparatively low (e.g. 0.09 and
466 0.07 μmol L^{-1}). This implies a potential role of phosphate limitation in the shift in diazotroph
467 community composition. UCYN-A1 and γ-24774A11 both appear to be broadly distributed
468 throughout low nutrient marine waters (Thompson et al., 2014; Langlois et al., 2015), and it
469 has been hypothesised that these taxa thrive in oligotrophic conditions (Church et al., 2008;
470 Krupke et al., 2014). In line with our findings in the ATS and Coral Sea, Moisander et al.
471 (2014) recently demonstrated that γ-24774A11 was significantly negatively correlated to
472 soluble reactive phosphorous in the western South Pacific. Taken together, our findings

suggest that UCYN-A and γ-24774A11 increase in relative abundance and activity when oligotrophic conditions prevail.

While no correlations were observed between the different diazotrophic groups and oxidised forms of N, USF N_2 fixation rates exhibited a moderate negative correlation to ammonium concentration, although this is unlikely to be due to an inhibitory effect, because concentrations observed here were below those expected to inhibit N_2 fixation (Knapp, 2012). It has been suggested that tropical Australian waters are constantly nitrogen limited (Condie and Dunn, 2006) and across all sites and depths measured, N:P ratios indicated an excess of phosphate relative to nitrate and ammonium ($N:P \leq 6$). This may confer a competitive advantage to diazotrophic taxa (Moutin et al., 2008; Knapp, 2012), and suggests that N_2 fixation could play an important role in helping to alleviate nitrogen limitation within this region.

However, it is notable that much of the variability between ATS and Coral Sea *nifH* profiles remained unexplained in our analysis, and despite combined analyses and stringent standardisation across samples, some rare OTUs in the DNA appeared highly active in the cDNA, potentially indicating a disconnect between relative organismal abundance and N_2 fixation activity at some locations. Therefore, other factors may have had a significant influence on diazotroph distribution and activity, for instance, dissolved iron (dFe) availability is known to limit marine N_2 fixation (Sohm et al., 2011) and dFe additions can stimulate diazotrophic activity (Moisander et al., 2012; Turk-Kubo et al., 2012). In the western South Pacific ocean, Moisander et al. (2012) demonstrated that the abundances of unicellular diazotrophs, including UCYN-A and γ-24774A11, increased substantially in response to dFe amendments, but also exhibited signs of iron and phosphorous co-limitation. While we did not measure dFe throughout the ATS and Coral Sea during the present study,

497 previous evidence suggests that concentrations of particulate Fe are relatively high in the
498 Timor region of the ATS (Waite et al., 1995), but dFe concentrations may be relatively low
499 (Sohm et al., 2008), and *Trichodesmium* colonies have been shown to experience Fe
500 limitation in this region (Kustka et al., 2003). While this indicates that dFe availability could
501 have influenced diazotroph distributions during our study, additional work exploring dFe
502 dynamics, and the potential influence on diazotroph diversity and activity in the ATS and
503 Coral Sea, is required to further understand the mechanisms structuring diazotroph
504 populations and N_2 fixation throughout these regions.

505 Despite the relatively low concentrations of dissolved inorganic nitrogen, primary production
506 peaks in both the ATS and Coral Sea during the Austral winter (Lyne and Hayes, 2005;
507 Brewer et al., 2007). It was during this season we observed a substantial increase in both
508 unicellular N_2 fixation and the relative abundance of heterotrophic *nifH* sequences. Primary
509 production estimates from the winter sampling are detailed elsewhere (Robinson et al. In
510 Prep.), however using this data we calculated that wintertime USF in the ATS and Coral Sea
511 could supply up to 46 and 42 % respectively of the N required to sustain biomass assimilation
512 from measured primary production rates (assuming Redfield ratios for particulate matter).
513 Thus we propose that primary production here may be enhanced by the influx of newly fixed
514 N mediated by heterotrophic diazotrophs. While it has been argued that the abundances of
515 heterotrophic N_2 fixing bacteria in oceanic environments are not considered sufficient to
516 account for measured rates of N_2 fixation (Turk-Kubo et al., 2013), a recent large-scale
517 analysis of the abundance and distribution of marine γ–proteobacterial *nifH*, indicates that
518 this phylotype could play a significant role in oceanic N_2 fixation (Langlois et al., 2015). It
519 must be noted that the fate of N fixed by marine heterotrophic diazotrophs has not yet been
520 determined, and as such direct evidence of production supported by heterotrophic N_2 fixation
521 is lacking. However, our limited data suggests that heterotrophic diazotrophs are an important

522 component of N_2 fixing populations throughout tropical northern Australia, and that they may
523 contribute to relatively high USF rates of N_2 fixation. Given the apparent importance of
524 heterotrophic diazotrophs in our study region, future research determining the ultimate fate of
525 N fixed by these heterotrophs will be valuable for estimating the extent to which these
526 populations ultimately influence pools of bioavailable N and support primary production.

527 Our study has shown that the composition and activity of diazotrophs in Australia's tropical
528 waters are highly variable across shelf and open ocean environments. Overall, our rate
529 measurements confirm that diazotroph activity is an important process here, but our
530 molecular and statistical analyses suggests that the distinct physicochemical characteristics of
531 these waters drive heterogeneity in populations of photoautotrophic, photoheterotrophic and
532 heterotrophic N_2 fixing bacteria. This heterogeneity in turn leads to substantial changes in
533 rates of N_2 fixation and the subsequent addition of newly fixed N to the ocean. As such,
534 spatial (even within relatively localized boundaries) and seasonal shifts in diazotroph
535 diversity and activity must be considered in future regional and global marine N cycle
536 budgets and modelling efforts. This can only be achieved by further attempts to more
537 precisely map marine diazotrophic processes with increased spatiotemporal resolution.

538

539

540 Acknowledgements

541 We gratefully thank the scientific crew, captain and scientists on-board the *R/V Southern*
542 *Surveyor* during ss2012_t07 and ss2013_t03 for assistance with sampling and nutrient sample
543 analyses. This research was supported by the Australian Research Council Discovery Grant

Scheme (DP120102764 to JS and MB, DP1092892 to M.D, FT130100218 to JS, and DP0988002 to MB).

Conflict of Interest Statement

The authors declare no conflict of interest.

563 References

564 Alongi, D. (editor), Edyvane, K., do Ceu Guterres, M., Pranowo, W., Wirasantosa, S., and
565 Wasson, R. (2011) Biophysical profile of the Arafura and Timor Seas Jakarta.

566 Benavides, M., Agawin, N., Arístegui, J., Peene, J., and Stal, L. (2013) Dissolved organic
567 nitrogen and carbon release by a marine unicellular diazotrophic cyanobacterium. *Aquat.*
568 *Microb. Ecol.* **69**: 69–80.

569 Benavides, M., Bronk, D.A., Agawin, N.S.R., Pérez-Hernández, M.D., Hernández-Guerra,
570 A., and Arístegui, J. (2013) Longitudinal variability of size-fractionated N2 fixation and
571 DON release rates along 24.5°N in the subtropical North Atlantic. *J. Geophys. Res.*
572 *Ocean.* **118**: 3406–3415.

573 Benjamini, Y. and Hochberg, Y. (1995) Controlling the false discovery rate: a practical and
574 powerful approach to multiple testing. *J. R. Stat. Soc. Ser. B* **57**: 289–300.

575 Bombar, D., Turk-Kubo, K. a, Robidart, J., Carter, B.J., and Zehr, J.P. (2013) Non-
576 cyanobacterial nifH phylotypes in the North Pacific Subtropical Gyre detected by flow-
577 cytometry cell sorting. *Environ. Microbiol. Rep.* **5**: 705–15.

578 Bonnet, S., Biegala, I.C., Dutrieux, P., Slemons, L.O., and Capone, D.G. (2009) Nitrogen
579 fixation in the western equatorial Pacific: Rates, diazotrophic cyanobacterial size class
580 distribution, and biogeochemical significance. *Global Biogeochem. Cycles* **23**: 1–13.

581 Brewer, D., Flynn, A., Skewes, T., Corfield, J., Pearson, B., Alawo, J., and Young, J. (2007)
582 Ecosystems of the East Marine Planning Region CSIRO, Cleveland.

583 Burford, M. a., Rothlisberg, P.C., and Revill, A.T. (2009) Sources of nutrients driving
584 production in the Gulf of Carpentaria, Australia: a shallow tropical shelf system. *Mar.*
585 *Freshw. Res.* **60**: 1044.

586 Burford, M., Rothlisberg, P., and Wang, Y. (1995) Spatial and temporal distribution of
587 tropical phytoplankton species and biomass in the Gulf of Carpentaria, Australia. *Mar.*
588 *Ecol. Prog. Ser.* **118**: 255–266.

589 Capone, D., Zehr, J., Paerl, H., Bergman, B., and Carpenter, E. (1997) Trichodesmium, a
590 globally significant marine cyanobacterium. *Science.* **276**: 1221–1229.

591 Capone, D.G., Burns, J., Montoya, J.P., Subramaniam, A., Mahaffey, C., Gunderson, T., et al.
592 (2005) Nitrogen fixation by Trichodesmium spp.: An important source of new nitrogen
593 to the tropical and subtropical North Atlantic Ocean. *Global Biogeochem. Cycles* **19**:
594 GB2024.

595 Caporaso, J., Kuczynski, J., Stombaugh, J., Bittinger, K., Bushman, F., Costello, E.K., et al.
596 (2010) QIIME allows analysis of high-throughput community sequencing data. *Nat.*
597 *Methods* **7**: 335–336.

598 Ceccarelli, D. (2011) Australia' s Coral Sea A Biophysical Profile. *Rep. Prot. our Coral Sea*
599 *Coalit.*

600 Church, M., Bjorkman, K., Karl, D., Saito, M.A., and Zehr, J. (2008) Regional distributions
601 of nitrogen-fixing bacteria in the Pacific Ocean. *Limnol. Oceanogr.* **53**: 63–77.

602 Church, M.J., Mahaffey, C., Letelier, R.M., Lukas, R., Zehr, J.P., and Karl, D.M. (2009)
603 Physical forcing of nitrogen fixation and diazotroph community structure in the North
604 Pacific subtropical gyre. *Global Biogeochem. Cycles* **23**: GB2020.

605 Clarke, K. (1993) Non-parametric multivariate analyses of changes in community structure.
606 *Aust. J. Ecol.* **18**: 117–143.

607 Clarke, K. and Warwick, R. (2001) Change in marine communities: an approach to statistical
608 analysis and interpretation 2nd Edition PRIMER-E Ltd: Plymouth.

609 Condie, S.A. and Dunn, J.R. (2006) Seasonal characteristics of the surface mixed layer in the
610 Australasian region: implications for primary production regimes and biogeography.
611 *Mar. Freshw. Res.* **57**: 569.

612 Dekaezemacker, J., Bonnet, S., Grosso, O., Moutin, T., Bressac, M., and Capone, D.G.
613 (2013) Evidence of active dinitrogen fixation in surface waters of the eastern tropical
614 South Pacific during El Niño and La Niña events and evaluation of its potential nutrient
615 controls. *Global Biogeochem. Cycles* **27**: 768–779.

616 Dowd, S.E., Callaway, T.R., Wolcott, R.D., Sun, Y., McKeehan, T., Hagevoort, R.G., and
617 Edrington, T.S. (2008) Evaluation of the bacterial diversity in the feces of cattle using
618 16S rDNA bacterial tag-encoded FLX amplicon pyrosequencing (bTEFAP). *BMC*
619 *Microbiol.* **8**: 125.

620 Edgar, R.C. (2010) Search and clustering orders of magnitude faster than BLAST.
621 *Bioinformatics* **26**: 2460–1.

622 Farnelid, H., Andersson, A.F., Bertilsson, S., Al-Soud, W.A., Hansen, L.H., Sørensen, S., et
623 al. (2011) Nitrogenase gene amplicons from global marine surface waters are dominated
624 by genes of non-cyanobacteria. *PLoS One* **6**: e19223.

625 Farnelid, H., Bentzon-Tilia, M., Andersson, A.F., Bertilsson, S., Jost, G., Labrenz, M., et al.
626 (2013) Active nitrogen-fixing heterotrophic bacteria at and below the chemocline of the
627 central Baltic Sea. *ISME J.* 1–11.

628 Fish, J.A., Chai, B., Wang, Q., Sun, Y., Brown, C.T., Tiedje, J.M., and Cole, J.R. (2013)
629 FunGene: the functional gene pipeline and repository. *Front. Microbiol.* **4**: 291.

630 Foster, R. a, Subramaniam, A., and Zehr, J.P. (2009) Distribution and activity of diazotrophs
631 in the Eastern Equatorial Atlantic. *Environ. Microbiol.* **11**: 741–50.

632 Foster, R.A., Kuypers, M.M.M., Vagner, T., Paerl, R.W., Musat, N., and Zehr, J.P. (2011)
633 Nitrogen fixation and transfer in open ocean diatom-cyanobacterial symbioses. *ISME J.*
634 **5**: 1484–93.

635 Frias-Lopez, J., Shi, Y., Tyson, G.W., Coleman, M.L., Schuster, S.C., Chisholm, S.W., and
636 Delong, E.F. (2008) Microbial community gene expression in ocean surface waters.
637 *Proc. Natl. Acad. Sci. U. S. A.* **105**: 3805–10.

638 Glibert, P. and Bronk, D. (1994) Release of dissolved organic nitrogen by marine
639 diazotrophic cyanobacteria, Trichodesmium spp. *Appl. Environ. Microbiol.* **60**: 3996–
640 4000.

641 Goebel, N.L., Turk, K.A., Achilles, K.M., Paerl, R., Hewson, I., Morrison, A.E., et al. (2010)
642 Abundance and distribution of major groups of diazotrophic cyanobacteria and their
643 potential contribution to N2 fixation in the tropical Atlantic Ocean. *Environ. Microbiol.*
644 **12**: 3272–3289.

645 Großkopf, T., Mohr, W., Baustian, T., Schunck, H., Gill, D., Kuypers, M.M.M., et al. (2012)
646 Doubling of marine dinitrogen-fixation rates based on direct measurements. *Nature* **488**:
647 361–364.

648 Hagino, K., Onuma, R., Kawachi, M., and Horiguchi, T. (2013) Discovery of an
649 Endosymbiotic Nitrogen-Fixing Cyanobacterium UCYN-A in Braarudosphaera
650 bigelowii (Prymnesiophyceae). *PLoS One* **8**: e81749.

651 Hallegraeff, G. and Jeffrey, S. (1984) Tropical phytoplankton species and pigments of
652 continental shelf waters of north and north-west Australia. *Mar. Ecol. Prog. Ser.* **20**: 59–
653 74.

654 Halm, H., Lam, P., Ferdelman, T.G., Lavik, G., Dittmar, T., LaRoche, J., et al. (2012)
655 Heterotrophic organisms dominate nitrogen fixation in the South Pacific Gyre. *ISME J.*
656 **6**: 1238–49.

657 Heller, P., Tripp, H.J., Turk-Kubo, K., and Zehr, J.P. (2014) ARBitrator: A software pipeline
658 for on-demand retrieval of auto-curated nifH sequences from GenBank. *Bioinformatics*
659 **30**: 1–8.

660 Karl, D.M., Church, M.J., Dore, J.E., Letelier, R.M., and Mahaffey, C. (2012) Predictable
661 and efficient carbon sequestration in the North Pacific Ocean supported by symbiotic
662 nitrogen fixation. *Proc. Natl. Acad. Sci. U. S. A.* **109**: 1842–9.

663 Knapp, A.N. (2012) The sensitivity of marine N2 fixation to dissolved inorganic nitrogen.
664 *Front. Microbiol.* **3**: 374.

665 Krupke, A., Lavik, G., Halm, H., Fuchs, B.M., Amann, R.I., and Kuypers, M.M.M. (2014)
666 Distribution of a consortium between unicellular algae and the N2 fixing
667 cyanobacterium UCYN-A in the North Atlantic Ocean. *Environ. Microbiol.*

668 Krupke, A., Musat, N., Laroche, J., Mohr, W., Fuchs, B.M., Amann, R.I., et al. (2013) In situ
669 identification and N2 and C fixation rates of uncultivated cyanobacteria populations.
670 *Syst. Appl. Microbiol.* **36**: 259–71.

671 Kustka, A., Sanudo-Wilhelmy, S., Carpenter, E., Capone, D., Burns, J., and Sunda, W. (2003)
672 Iron requirements for dinitrogen-and ammonium-supported growth in cultures of

673 Trichodesmium (IMS 101): Comparison with nitrogen fixation rates and iron: carbon
674 ratios of field populations. *Limnol. Oceanogr.* **48**: 1869–1884.

675 Langlois, R., Großkopf, T., Mills, M., Takeda, S., and LaRoche, J. (2015) Widespread
676 Distribution and Expression of Gamma A (UMB), an Uncultured, Diazotrophic, γ-
677 Proteobacterial nifH Phylotype. *PLoS One* **10**: e0128912.

678 Langlois, R., LaRoche, J., and Raab, P. (2005) Diazotrophic diversity and distribution in the
679 tropical and subtropical Atlantic Ocean. *Appl. Environ. Microbiol.* **71**: 7910–7919.

680 Langlois, R.J., Hümmer, D., and LaRoche, J. (2008) Abundances and distributions of the
681 dominant nifH phylotypes in the Northern Atlantic Ocean. *Appl. Environ. Microbiol.* **74**:
682 1922–31.

683 Legendre, P. and Anderson, M. (1999) Distance-based redundancy analysis: testing
684 multispecies responses in multifactorial ecological experiments. *Ecol. Monogr.* **69**: 1–
685 24.

686 Luo, Y.-W., Lima, I.D., Karl, D.M., Deutsch, C. a., and Doney, S.C. (2014) Data-based
687 assessment of environmental controls on global marine nitrogen fixation.
688 *Biogeosciences* **11**: 691–708.

689 Lyne, V. and Hayes, D. (2005) Pelagic Regionalisation: National Marine Bioregionalisation
690 Intgration Project Hobart.

691 Mazard, S., Fuller, N., Orcutt, K., Bridle, O., and Scanlan, D. (2004) PCR analysis of the
692 distribution of unicellular cyanobacterial diazotrophs in the Arabian Sea. *Appl. Environ.*
693 *Microbiol.* **70**: 7355–7364.

694 McArdle, B. and Anderson, M. (2001) Fitting multivariate models to community data: a
695 comment on distance-based redundancy analysis. *Ecology* **82**: 290–297.

696 McKinnon, A., Carleton, J., and Duggan, S. (2011) Determinants of pelagic metabolism in
697 the Timor Sea during the inter-monsoon period. *Mar. Freshw. Res.* **62**: 130–140.

698 Messer, L., Doubell, M., Jeffries, T., Brown, M., and Seymour, J. (2015) Prokaryotic and
699 diazotrophic population dynamics within a large oligotrophic inverse estuary. *Aquat.*
700 *Microb. Ecol.* **74**: 1–15.

701 Mohr, W., Grosskopf, T., Wallace, D.W.R., and LaRoche, J. (2010) Methodological
702 underestimation of oceanic nitrogen fixation rates. *PLoS One* **5**: e12583.

703 Moisander, P.H., Beinart, R. a, Voss, M., and Zehr, J.P. (2008) Diversity and abundance of
704 diazotrophic microorganisms in the South China Sea during intermonsoon. *ISME J.* **2**:
705 954–67.

706 Moisander, P.H., Beinart, R.A., Hewson, I., White, A.E., Johnson, K.S., Carlson, C.A., et al.
707 (2010) Unicellular cyanobacterial distributions broaden the oceanic N2 fixation domain.
708 *Science* **327**: 1512–4.

709 Moisander, P.H., Serros, T., Paerl, R.W., Beinart, R. a, and Zehr, J.P. (2014)
710 Gammaproteobacterial diazotrophs and nifH gene expression in surface waters of the
711 South Pacific Ocean. *ISME J.* 1–12.

712 Moisander, P.H., Zhang, R., Boyle, E. a, Hewson, I., Montoya, J.P., and Zehr, J.P. (2012)
713 Analogous nutrient limitations in unicellular diazotrophs and Prochlorococcus in the
714 South Pacific Ocean. *ISME J.* **6**: 733–44.

715 Monteiro, F.M., Follows, M.J., and Dutkiewicz, S. (2010) Distribution of diverse nitrogen
716 fixers in the global ocean. *Global Biogeochem. Cycles* **24**: 1–16.

717 Montoya, J., Holl, C., Zehr, J., and Hansen, A. (2004) High rates of N2 fixation by
718 unicellular diazotrophs in the oligotrophic Pacific Ocean. *Nature* **430**: 1027–1031.

719 Montoya, J.P., Voss, M., Kahler, P., and Capone, D.G. (1996) A Simple, High-Precision,
720 High-Sensitivity Tracer Assay for N2 Fixation. *Appl. Environ. Microbiol.* **62**: 986–93.

721 Moutin, T., Karl, D., Duhamel, S., Rimmelin, P., Raimbault, P., Van Mooy, B., and Claustre,
722 H. (2008) Phosphate availability and the ultimate control of new nitrogen input by
723 nitrogen fixation in the tropical Pacific Ocean. *Biogeosciences* **5**: 95–109.

724 Mulholland, M.R. (2007) The fate of nitrogen fixed by diazotrophs in the ocean.
725 *Biogeosciences* **4**: 37–51.

726 Penton, C.R., Johnson, T.A., Quensen, J.F., Iwai, S., Cole, J.R., and Tiedje, J.M. (2013)
727 Functional genes to assess nitrogen cycling and aromatic hydrocarbon degradation:
728 primers and processing matter. *Front. Microbiol.* **4**: 279.

729 Qu, T. and Lindstrom, E.J. (2002) A Climatological Interpretation of the Circulation in the
730 Western South Pacific. *J. Phys. Oceanogr.* **32**: 2492–2508.

731 Raes, E., Waite, A., McInnes, A., Olsen, H., Nguyen, H., Hardman-Mountford, N., and
732 Thompson, P. (2014) Changes in latitude and dominant diazotrophic community alter
733 N2 fixation. *Mar. Ecol. Prog. Ser.* **516**: 85–102.

734 Raimbault, P. and Garcia, N. (2008) Evidence for efficient regenerated production and
735 dinitrogen fixation in nitrogen-deficient waters of the South Pacific Ocean: impact on
736 new and export production estimates. *Biogeosciences* **5**: 323–338.

737 Rees, A.P., Law, C.S., and Woodward, E.M.S. (2006) High rates of nitrogen fixation during
738 an in-situ phosphate release experiment in the Eastern Mediterranean Sea. *Geophys. Res.*
739 *Lett.* **33**: L10607.

740 Reshef, D., Reshef, Y., and Finucane, H. (2011) Detecting novel associations in large data
741 sets. *Science.* **334**: 1518–1524.

742 Robidart, J.C., Church, M.J., Ryan, J.P., Ascani, F., Wilson, S.T., Bombar, D., et al. (2014)
743 Ecogenomic sensor reveals controls on N2-fixing microorganisms in the North Pacific
744 Ocean. *ISME J.* 1175–1185.

745 Sañudo-Wilhelmy, S. a, Kustka, a B., Gobler, C.J., Hutchins, D. a, Yang, M., Lwiza, K., et al.
746 (2001) Phosphorus limitation of nitrogen fixation by Trichodesmium in the central
747 Atlantic Ocean. *Nature* **411**: 66–69.

748 Smoot, M.E., Ono, K., Ruscheinski, J., Wang, P.-L., and Ideker, T. (2011) Cytoscape 2.8:
749 new features for data integration and network visualization. *Bioinformatics* **27**: 431–2.

750 Sohm, J. a., Mahaffey, C., and Capone, D.G. (2008) Assessment of relative phosphorus
751 limitation of Trichodesmium spp. in the North Pacific, North Atlantic, and the north
752 coast of Australia. *Limnol. Oceanogr.* **53**: 2495–2502.

753 Sohm, J.A., Webb, E.A., and Capone, D.G. (2011) Emerging patterns of marine nitrogen
754 fixation. *Nat. Rev. Microbiol.* **9**: 499–508.

755 Stewart, F.J., Ottesen, E.A., and DeLong, E.F. (2010) Development and quantitative analyses
756 of a universal rRNA-subtraction protocol for microbial metatranscriptomics. *ISME J.* **4**:
757 896–907.

758 Thompson, A., Carter, B.J., Turk-Kubo, K., Malfatti, F., Azam, F., and Zehr, J.P. (2014)
759 Genetic diversity of the unicellular nitrogen-fixing cyanobacteria UCYN-A and its
760 prymnesiophyte host. *Environ. Microbiol.* doi:10.1111/1462–2920.12490.

761 Thompson, A.W., Foster, R.A., Krupke, A., Carter, B.J., Musat, N., Vaulot, D., et al. (2012)
762 Unicellular cyanobacterium symbiotic with a Single-Celled Eukaryotic Alga. *Science*
763 **337**: 1546–1550.

764 Turk-Kubo, K. a, Karamchandani, M., Capone, D.G., and Zehr, J.P. (2013) The paradox of
765 marine heterotrophic nitrogen fixation: abundances of heterotrophic diazotrophs do not
766 account for nitrogen fixation rates in the Eastern Tropical South Pacific. *Environ.*
767 *Microbiol.*

768 Turk-Kubo, K.A., Achilles, K.M., Serros, T.R.C., Ochiai, M., Montoya, J.P., and Zehr, J.P.
769 (2012) Nitrogenase (nifH) gene expression in diazotrophic cyanobacteria in the Tropical
770 North Atlantic in response to nutrient amendments. *Front. Microbiol.* **3**: 386.

771 Waite, T.D., Szymczak, R., Espey, Q.I., and Furnas, M.J. (1995) Diel variations in iron
772 speciation in northern Australian shelf waters. *Mar. Chem.* **50**: 79–91.

773 Wang, Q., Quensen, J., Fish, J., Lee, T., Sun, Y., Tiedje, J., and Cole, J.R. (2013) Ecological
774 Patterns of nifH Genes in Four Terrestrial Climatic Zones Explored with Targeted
775 Metagenomics Using FrameBot, a New Informatics Tool. *MBio* **4**: e00592–13.

776 Westram, R., Baider, K., Prusse, E., Kuhmar, Y., Meirer, H., Glockner, F.O., and Ludwig, W.
777 (2011) ARB: a software environment for sequence data. In, Bruijn,F.J. (ed), *Handbook*
778 *of Molecular Microbial Ecology I: Metagenomics and Complementary Approaches*.
779 John Wiley & Sons, Inc, pp. 399–406.

780 Wilson, S.T., Böttjer, D., Church, M.J., and Karl, D.M. (2012) Comparative assessment of
781 nitrogen fixation methodologies, conducted in the oligotrophic North Pacific Ocean.
782 *Appl. Environ. Microbiol.* **78**: 6516–23.

783 Zani, S., Mellon, M., Collier, J., and Zehr, J. (2000) Expression of nifH genes in natural
784 microbial assemblages in Lake George, New York, detected by reverse transcriptase
785 PCR. *Appl. Environ. Microbiol.* **66**: 3119–3124.

786 Zehr, J., Jenkins, B., Short, S., and Steward, G. (2003) Nitrogenase gene diversity and
787 microbial community structure: a cross system comparison. *Environ. Microbiol.* **5**: 539–
788 554.

789 Zehr, J. and Turner, P. (2001) Nitrogen fixation: Nitrogenase genes and gene expression.
790 *Methods Microbiol.* **30**: 271–285.

791 Zehr, J.P. and Kudela, R.M. (2011) Nitrogen Cycle of the Open Ocean: From Genes to
792 Ecosystems. *Ann. Rev. Mar. Sci.* **3**: 197–225.

793

794

795 Figure Legends

Figure 1. Physical and chemical characteristics of surface waters sampled within the ATS (stations SS1-8; WS1-12) and Coral Sea (stations SS9-17; WS13-18) during the (A) spring and (B) winter. Note the different scales within and between A and B.

Figure 2. Mean N_2 fixation rates (± s.e., n = 3) performed by the whole community (WC) and
800 < 10 μm unicellular size fraction (USF) at the surface and chlorophyll maxima during the spring (SS; A) and winter (WS; B) transects.

Figure 3. Relative abundance of *nifH* OTUs recovered from community DNA (% sequences) at the surface and chlorophyll maxima during the spring (SS; A & B) and winter (WS; C & D) transects. In parentheses are the closest cultured representatives that share ≥ 90% amino
805 acid identity with the detected sequences.

Figure 4. Relative abundance of *nifH* transcripts detected in surface and chlorophyll maxima waters for spring (A & B respectively) and winter (C & D respectively) voyages.

Figure 5. Distance based redundancy analysis constrained by the significant ($P < 0.05$) explanatory environmental variables for the observed variation in *nifH* composition within
810 (A) DNA and (B) cDNA profiles in spring (S) and winter (W).

Figure 6. Network analysis demonstrating significant ($P < 0.01$) associations only, between (A) phosphate concentrations and (B) silicate concentrations, and other environmental variables as well as the relative abundance of expressed *nifH* OTUs. In addition, significant ($P < 0.01$) associations between (C) OTU4713 of the γ-24774A11 clade and (D) OTU6352
815 *Candidatus* Atelocyanobacterium thalassa (UCYN-A1), environmental data and the relative abundance of other expressed *nifH* OTUs are also shown. Circular nodes = *nifH* cDNA OTUs, the relative abundance is demonstrated by the relative size of the node; diamond

nodes = physical variables; square nodes = dissolved inorganic nutrients; hexagon nodes = photosynthetic pigments. Positive linear regressions between nodes are denoted by solid lines, negative linear regressions are dashed. Line colour represents the strength of the test statistic, MIC: high > 0.8 < 1 = blue; medium > 0.6 < 0.8 = green; low > 0.47 < 0.6 = black.

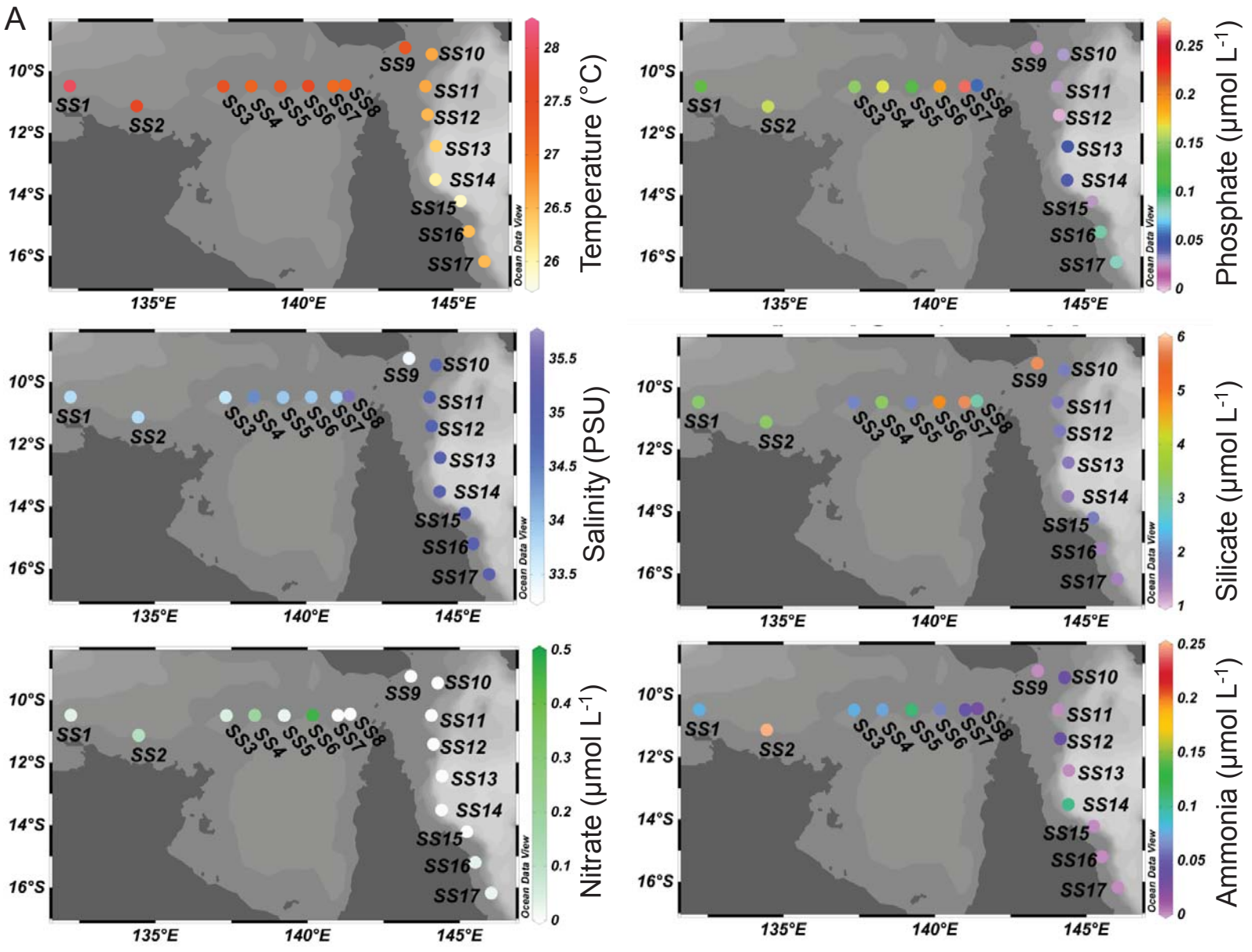
A
10°S
12°S
14°S
16°S
135°E
140°E
145°E
SS1
SS2
SS3
SS4
SS5
SS6
SS7
SS8
SS9
SS10
SS11
SS12
SS13
SS14
SS15
SS16
SS17
Ocean Data View
28
27.5
27
26.5
26
Temperature (°C)
0.25
0.2
0.15
0.1
0.05
0
Phosphate (µmol L-1)
35.5
35
34.5
34
33.5
Salinity (PSU)
6
5
4
3
2
1
Silicate (µmol L-1)
0.5
0.4
0.3
0.2
0.1
0
Nitrate (µmol L-1)
0.25
0.2
0.15
0.1
0.05
0
Ammonia (µmol L-1)

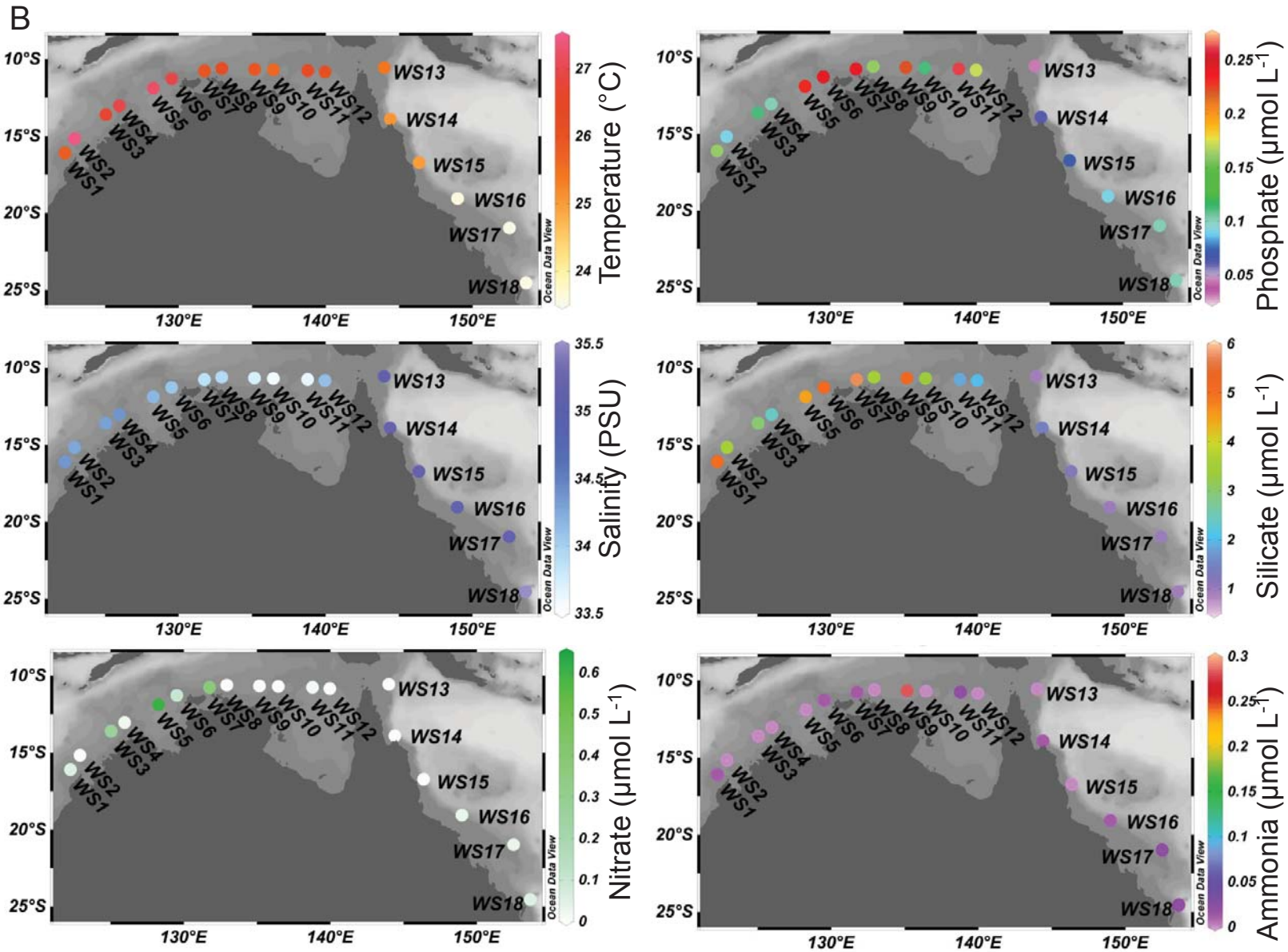
B
10°S
15°S
20°S
25°S
130°E
140°E
150°E
WS1
WS2
WS3
WS4
WS5
WS6
WS7
WS8
WS9
WS10
WS11
WS12
WS13
WS14
WS15
WS16
WS17
WS18
Ocean Data View
Temperature (°C)
27
26
25
24
Phosphate (µmol L-1)
0.25
0.2
0.15
0.1
0.05
Salinity (PSU)
35.5
35
34.5
34
33.5
Silicate (µmol L-1)
6
5
4
3
2
1
Nitrate (µmol L-1)
0.6
0.5
0.4
0.3
0.2
0.1
0
Ammonia (µmol L-1)
0.3
0.25
0.2
0.15
0.1
0.05
0

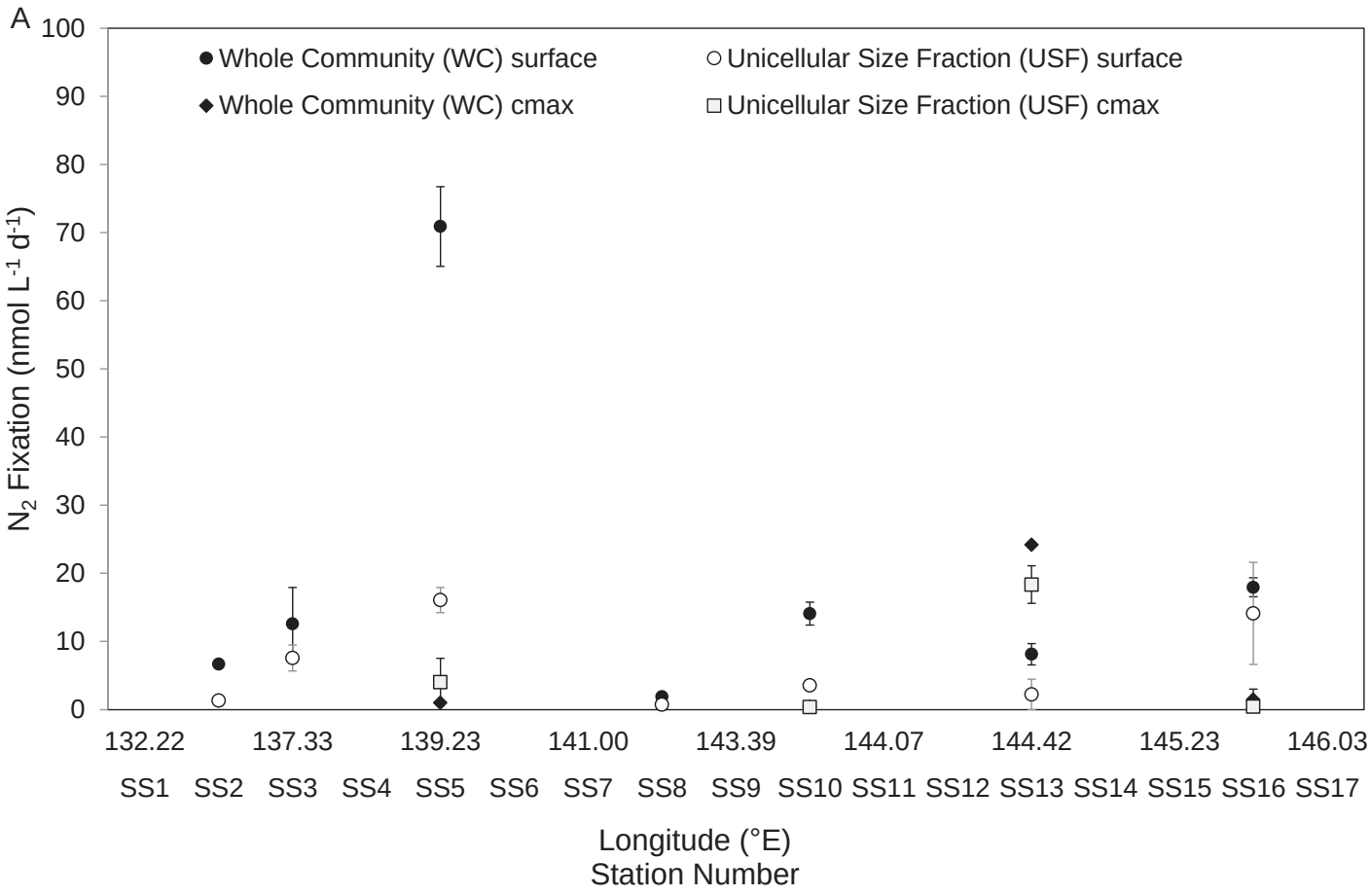
A
Whole Community (WC) surface
Unicellular Size Fraction (USF) surface
Whole Community (WC) cmax
Unicellular Size Fraction (USF) cmax
N_2 Fixation (nmol L^{-1} d^{-1})
100
90
80
70
60
50
40
30
20
10
0
132.22
137.33
139.23
141.00
143.39
144.07
144.42
145.23
146.03
SS1 SS2 SS3 SS4 SS5 SS6 SS7 SS8 SS9 SS10 SS11 SS12 SS13 SS14 SS15 SS16 SS17
Longitude (°E)
Station Number

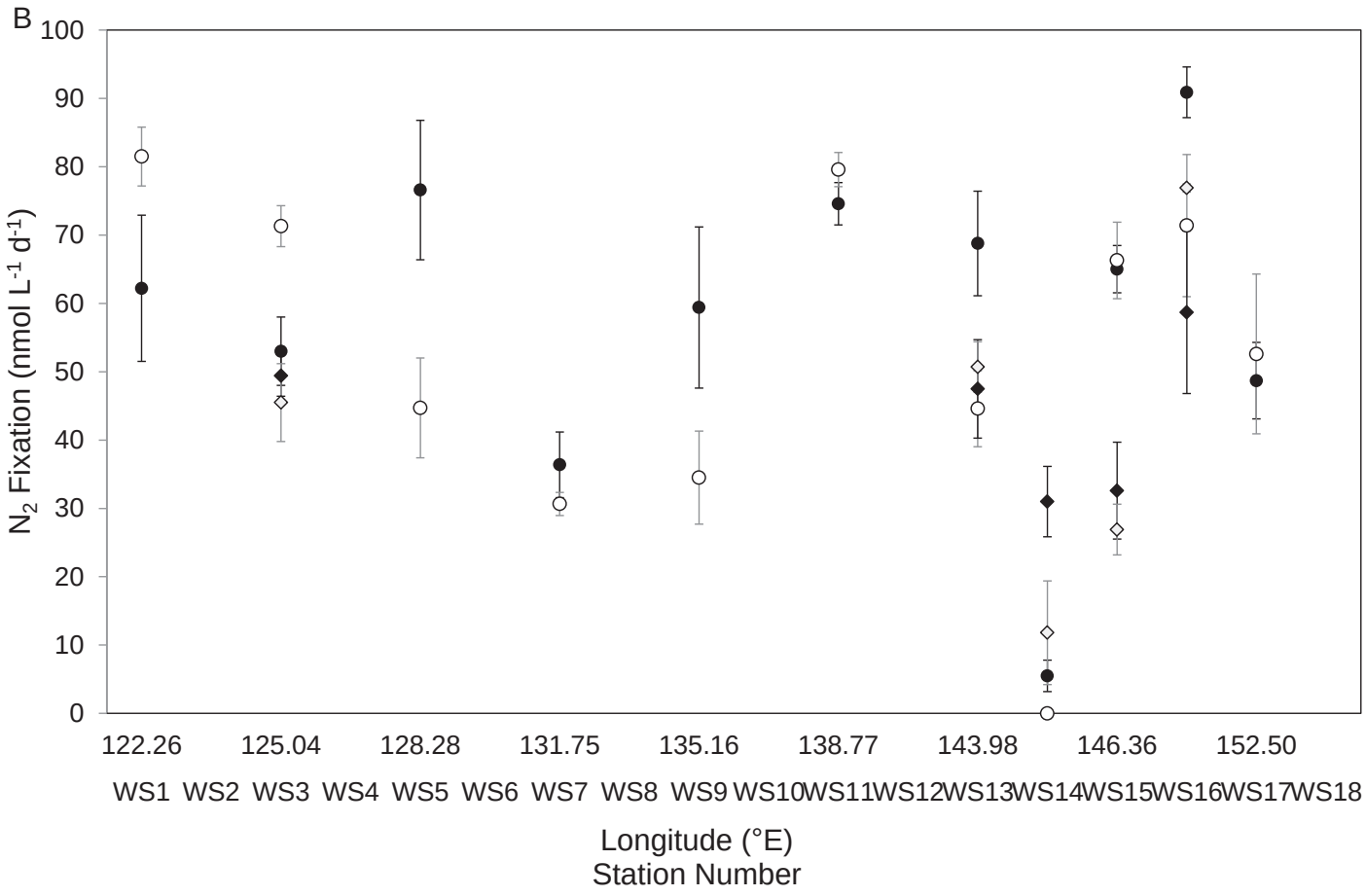
B
100
90
80
70
60
50
40
30
20
10
0
N_2 Fixation (nmol L^{-1} d^{-1})
122.26
125.04
128.28
131.75
135.16
138.77
143.98
146.36
152.50
WS1 WS2 WS3 WS4 WS5 WS6 WS7 WS8 WS9 WS10 WS11 WS12 WS13 WS14 WS15 WS16 WS17 WS18
Longitude (°E)
Station Number

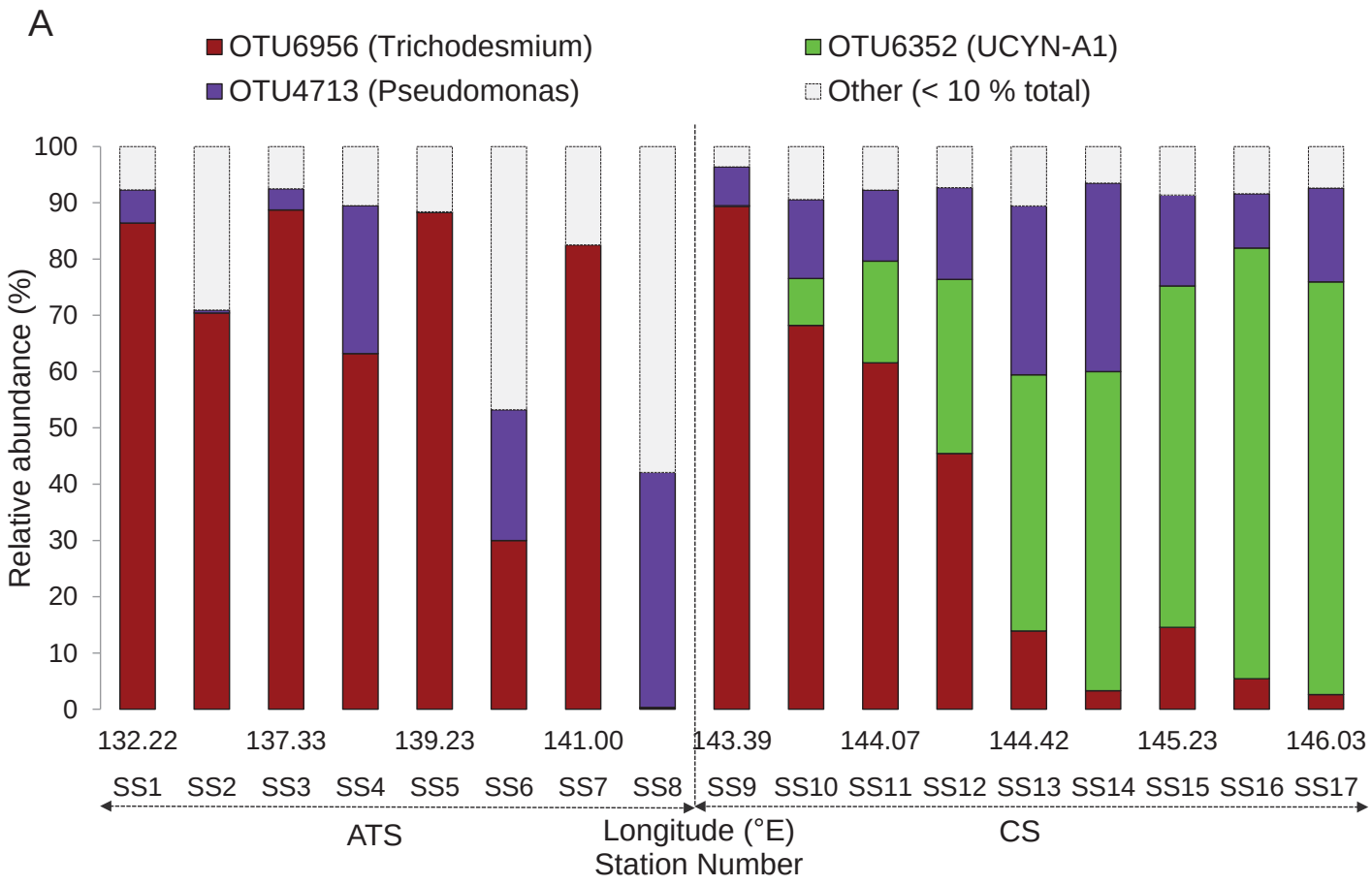
A
OTU6956 (Trichodesmium)
OTU6352 (UCYN-A1)
OTU4713 (Pseudomonas)
Other (< 10 % total)
Relative abundance (%)
100
90
80
70
60
50
40
30
20
10
0
132.22
137.33
139.23
141.00
143.39
144.07
144.42
145.23
146.03
SS1 SS2 SS3 SS4 SS5 SS6 SS7 SS8 SS9 SS10 SS11 SS12 SS13 SS14 SS15 SS16 SS17
ATS
CS
Longitude (°E)
Station Number

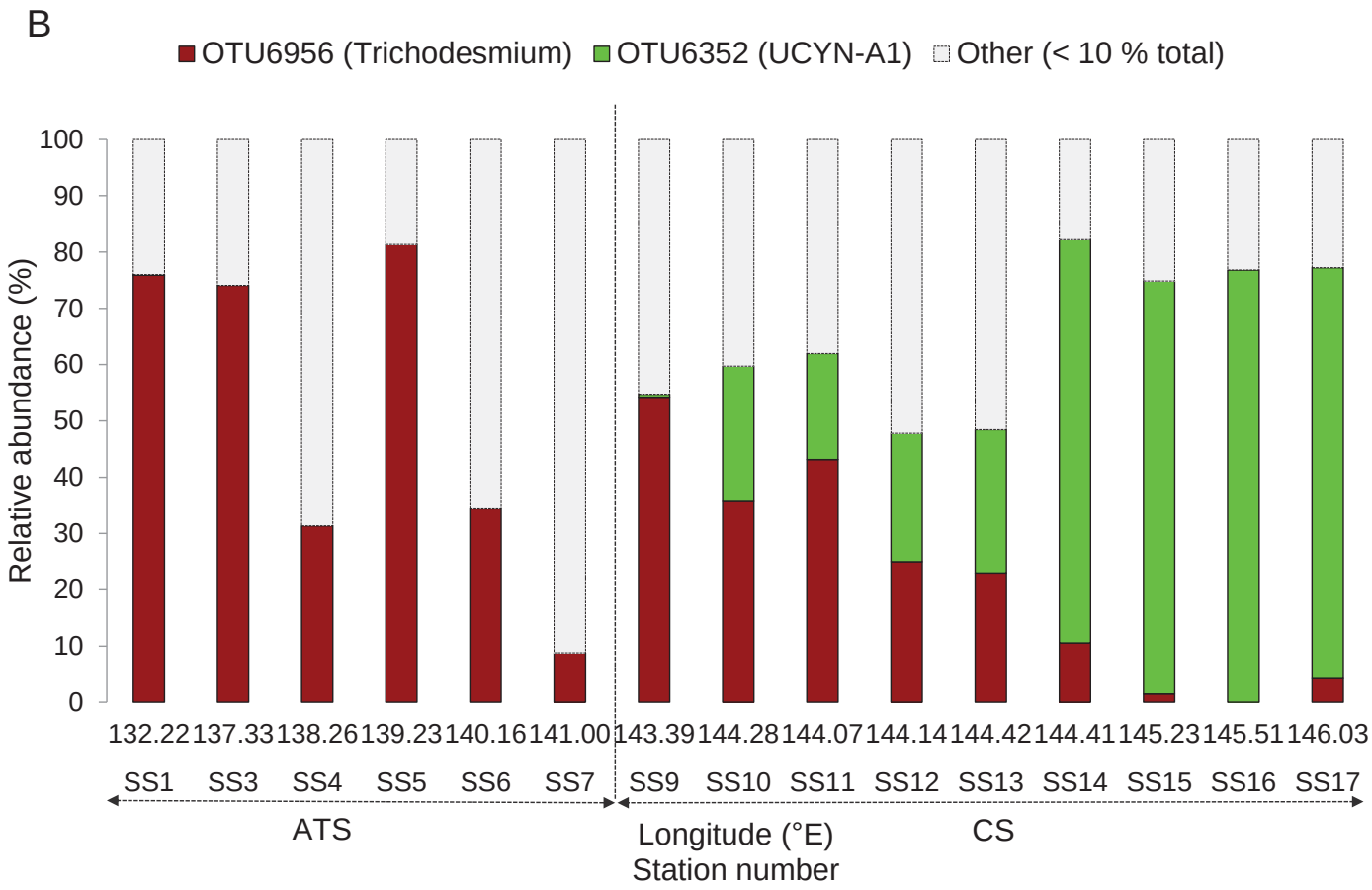
B
OTU6956 (Trichodesmium)
OTU6352 (UCYN-A1)
Other (< 10 % total)
Relative abundance (%)
100
90
80
70
60
50
40
30
20
10
0
132.22 137.33 138.26 139.23 140.16 141.00 143.39 144.28 144.07 144.14 144.42 144.41 145.23 145.51 146.03
SS1 SS3 SS4 SS5 SS6 SS7 SS9 SS10 SS11 SS12 SS13 SS14 SS15 SS16 SS17
ATS
CS
Longitude (°E)
Station number

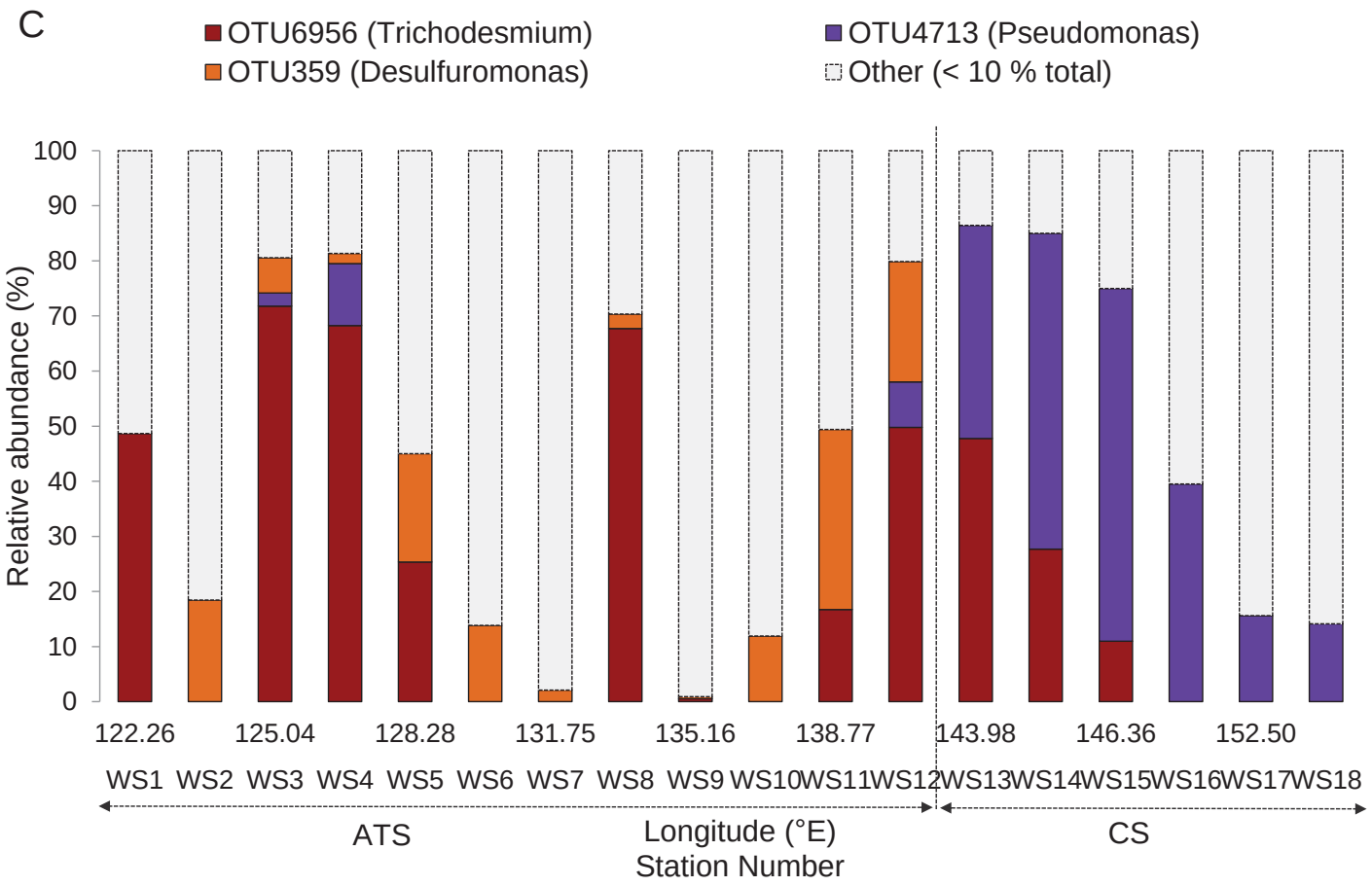
C
OTU6956 (Trichodesmium)
OTU4713 (Pseudomonas)
OTU359 (Desulfuromonas)
Other (< 10 % total)
Relative abundance (%)
100
90
80
70
60
50
40
30
20
10
0
122.26
125.04
128.28
131.75
135.16
138.77
143.98
146.36
152.50
WS1 WS2 WS3 WS4 WS5 WS6 WS7 WS8 WS9 WS10 WS11 WS12 WS13 WS14 WS15 WS16 WS17 WS18
ATS
Longitude (°E)
Station Number
CS

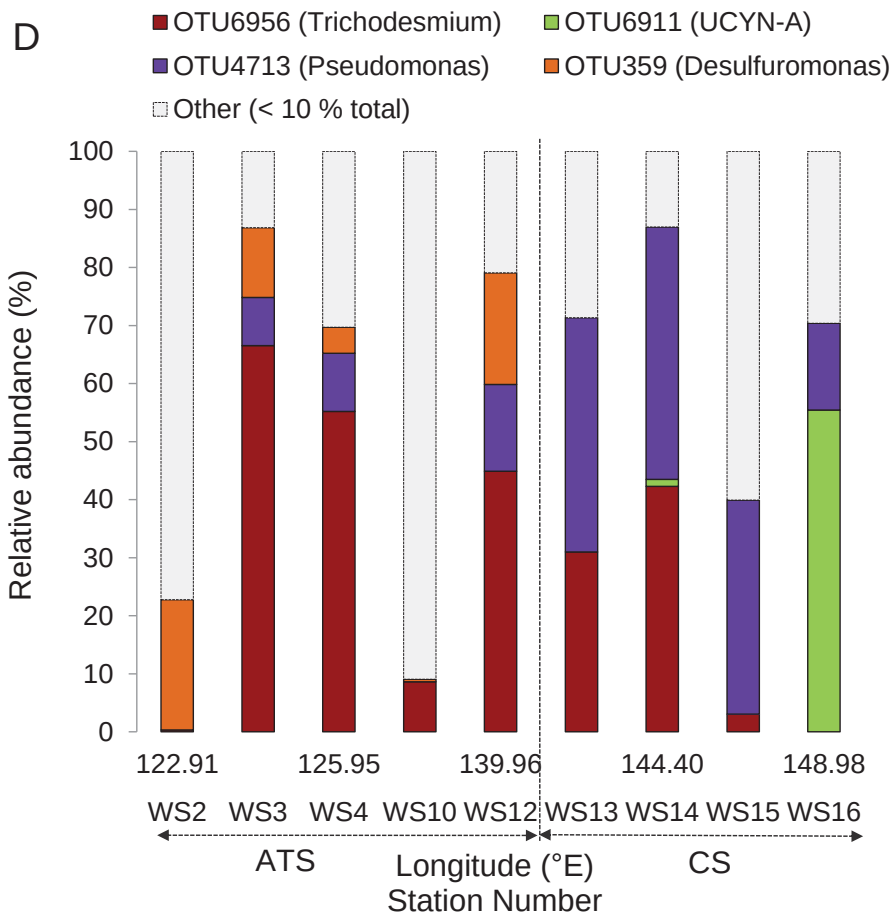
D
OTU6956 (Trichodesmium)
OTU6911 (UCYN-A)
OTU4713 (Pseudomonas)
OTU359 (Desulfuromonas)
Other (< 10 % total)
Relative abundance (%)
100
90
80
70
60
50
40
30
20
10
0
122.91
125.95
139.96
144.40
148.98
WS2 WS3 WS4 WS10 WS12 WS13 WS14 WS15 WS16
ATS
CS
Longitude (°E)
Station Number

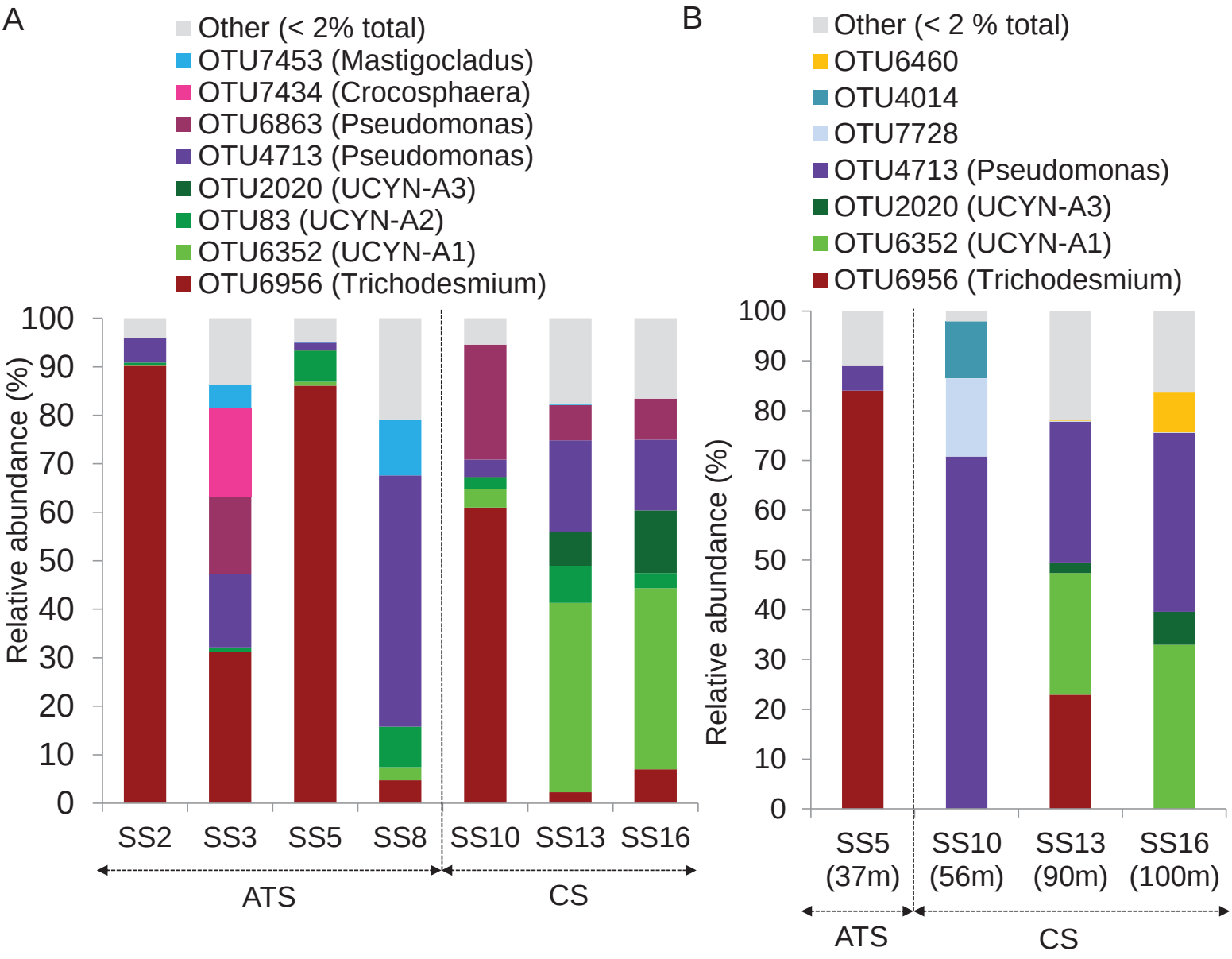
A
Other (< 2% total)
OTU7453 (Mastigocladus)
OTU7434 (Crocosphaera)
OTU6863 (Pseudomonas)
OTU4713 (Pseudomonas)
OTU2020 (UCYN-A3)
OTU83 (UCYN-A2)
OTU6352 (UCYN-A1)
OTU6956 (Trichodesmium)
Relative abundance (%)
100
90
80
70
60
50
40
30
20
10
0
SS2
SS3
SS5
SS8
SS10
SS13
SS16
ATS
CS
B
Other (< 2 % total)
OTU6460
OTU4014
OTU7728
OTU4713 (Pseudomonas)
OTU2020 (UCYN-A3)
OTU6352 (UCYN-A1)
OTU6956 (Trichodesmium)
Relative abundance (%)
100
90
80
70
60
50
40
30
20
10
0
SS5 (37m)
SS10 (56m)
SS13 (90m)
SS16 (100m)
ATS
CS

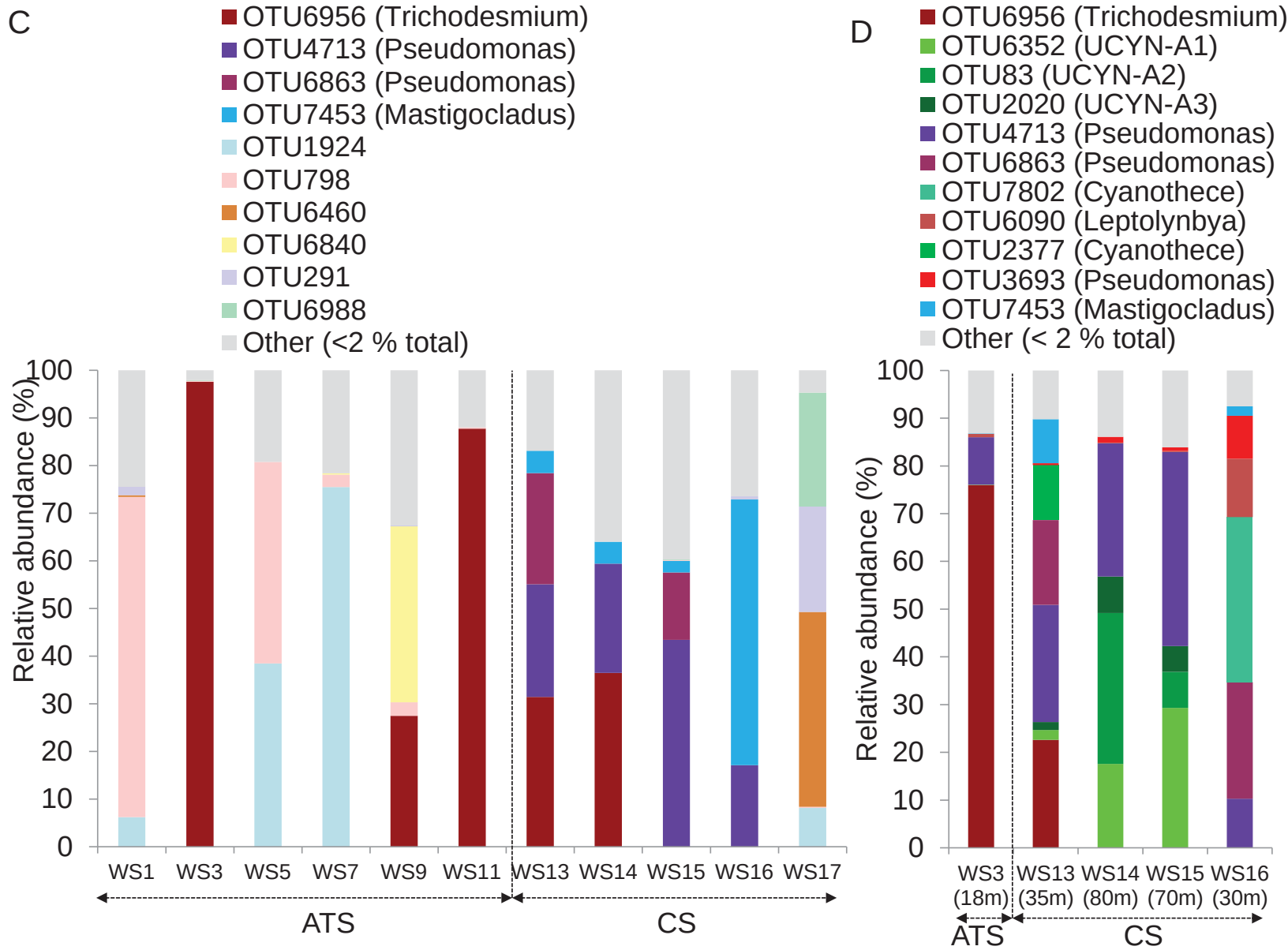
C
OTU6956 (Trichodesmium)
OTU4713 (Pseudomonas)
OTU6863 (Pseudomonas)
OTU7453 (Mastigocladus)
OTU1924
OTU798
OTU6460
OTU6840
OTU291
OTU6988
Other (<2 % total)
Relative abundance (%)
100
90
80
70
60
50
40
30
20
10
0
WS1
WS3
WS5
WS7
WS9
WS11
WS13
WS14
WS15
WS16
WS17
ATS
CS
D
OTU6956 (Trichodesmium)
OTU6352 (UCYN-A1)
OTU83 (UCYN-A2)
OTU2020 (UCYN-A3)
OTU4713 (Pseudomonas)
OTU6863 (Pseudomonas)
OTU7802 (Cyanothece)
OTU6090 (Leptolynbya)
OTU2377 (Cyanothece)
OTU3693 (Pseudomonas)
OTU7453 (Mastigocladus)
Other (< 2 % total)
Relative abundance (%)
100
90
80
70
60
50
40
30
20
10
0
WS3 (18m)
WS13 (35m)
WS14 (80m)
WS15 (70m)
WS16 (30m)
ATS
CS

A

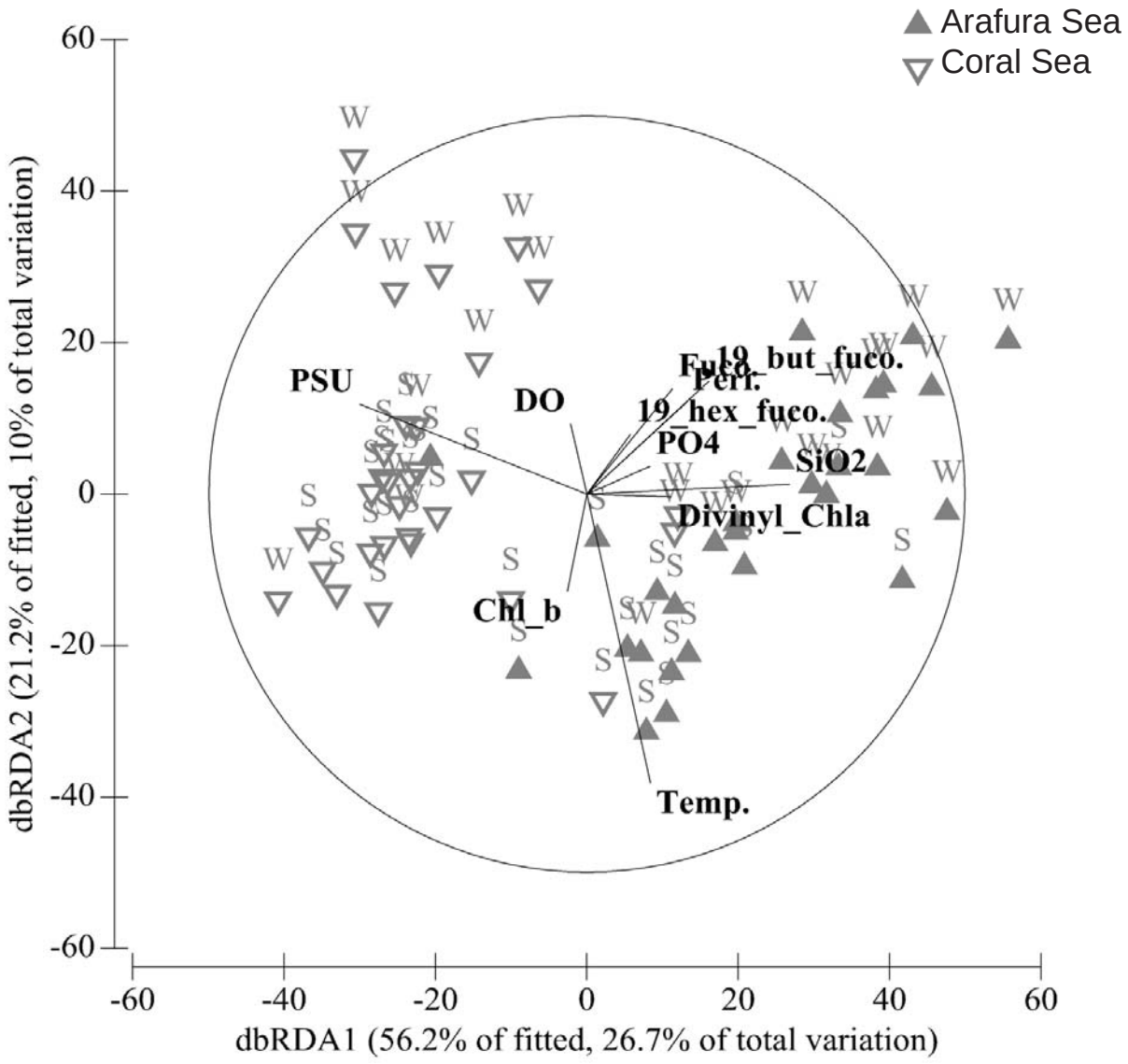
Arafura Sea
Coral Sea
PSU
DO
Fuco.
19_but_fuco.
Perl.
19_hex_fuco.
PO4
SiO2
Divinyl_Chla
Chl_b
Temp.
60
40
20
0
-20
-40
-60
-60
-40
-20
0
20
40
60
dbRDA2 (21.2% of fitted, 10% of total variation)
dbRDA1 (56.2% of fitted, 26.7% of total variation)

B

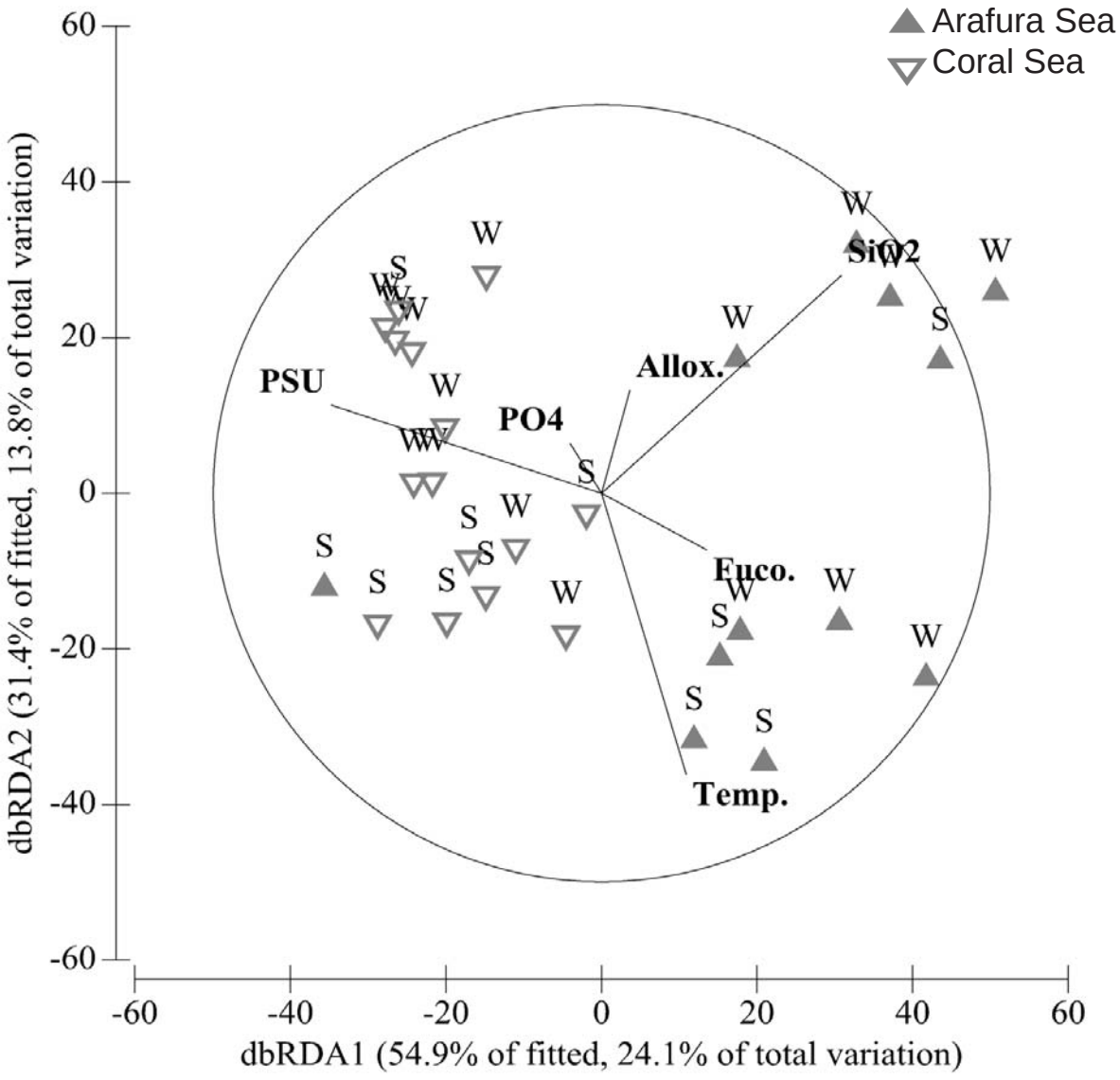
Arafura Sea
Coral Sea
PSU
PO4
Allox.
Fuco.
Temp.
dbRDA1 (54.9% of fitted, 24.1% of total variation)
dbRDA2 (31.4% of fitted, 13.8% of total variation)
60
40
20
0
-20
-40
-60
-60
-40
-20
0
20
40
60

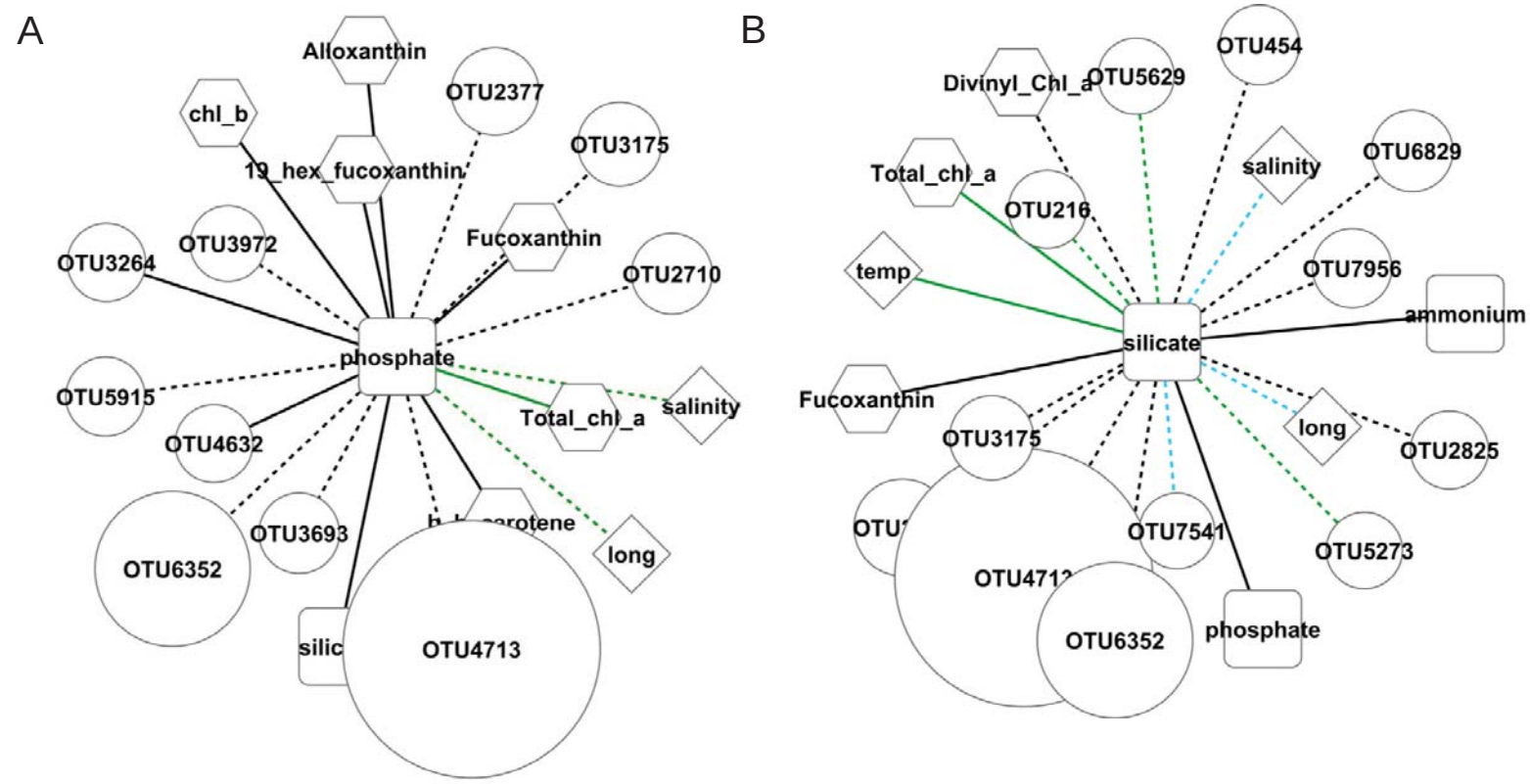
A
Alloxanthin
chl_b
OTU2377
OTU3175
19_hex_fucoxanthin
OTU3264
OTU3972
Fucoxanthin
OTU2710
phosphate
OTU5915
OTU4632
Total_chl_a
salinity
OTU6352
OTU3693
long
silic
OTU4713
B
OTU454
Divinyl_Chl_a
OTU5629
Total_chl_a
salinity
OTU6829
OTU216
temp
OTU7956
ammonium
silicate
Fucoxanthin
OTU3175
long
OTU2825
OTU7541
OTU5273
OTU6352
phosphate

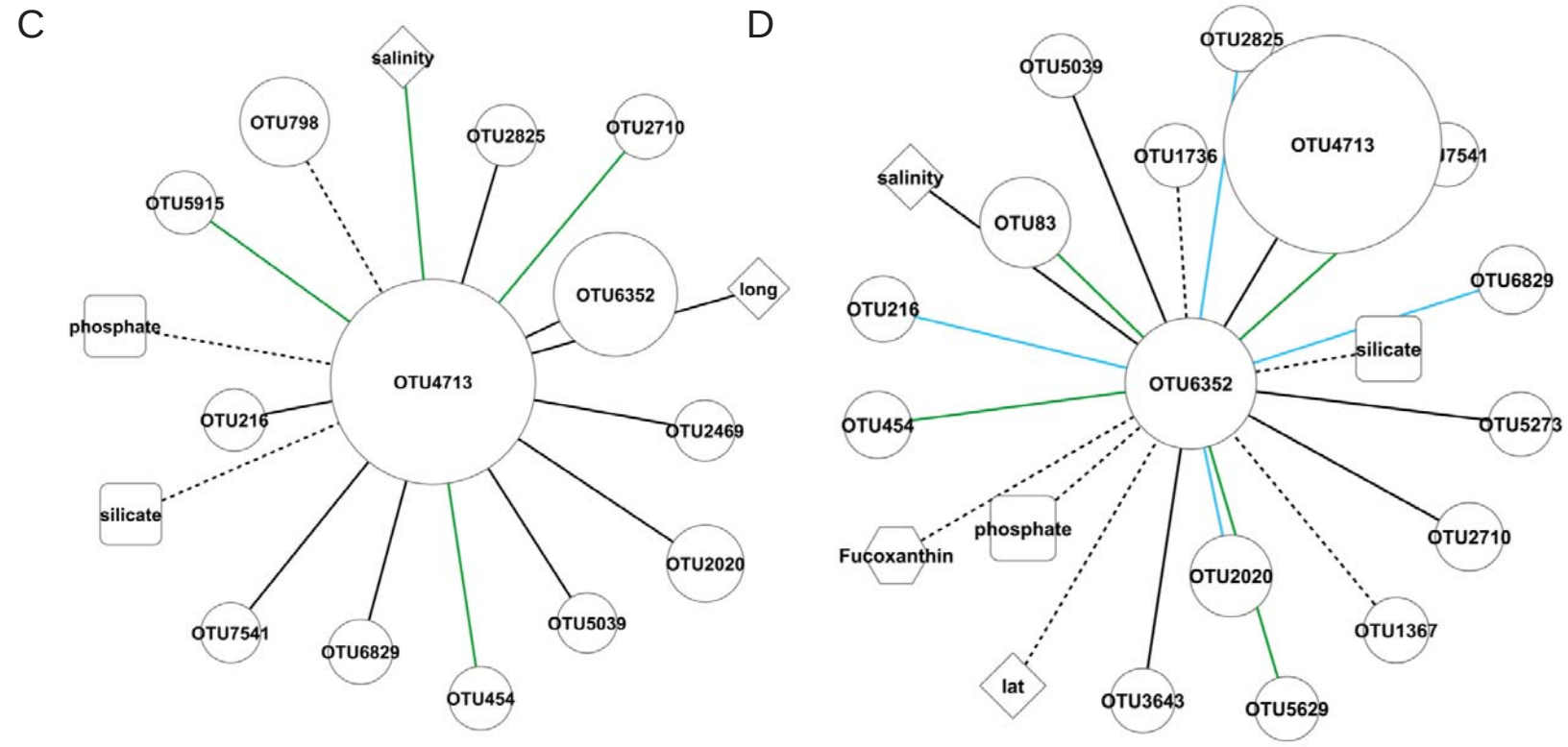
C
salinity
OTU798
OTU2825
OTU2710
OTU5915
OTU6352
long
phosphate
OTU4713
OTU216
OTU2469
silicate
OTU2020
OTU7541
OTU6829
OTU5039
OTU454
D
OTU2825
OTU5039
OTU1736
OTU4713
salinity
OTU83
OTU6829
OTU216
silicate
OTU6352
OTU454
OTU5273
Fucoxanthin
phosphate
OTU2710
OTU2020
OTU1367
lat
OTU3643
OTU5629